6-24-2024

STUDY OF POLYMER-ON-POLYMER COLD SPRAY DEPOSITION WINDOWS UNDER APPARENTLY SIMILAR CONDITIONS

Ülar Tiitma
Rowan University

STUDY OF POLYMER-ON-POLYMER COLD SPRAY DEPOSITION WINDOWS UNDER APPARENTLY SIMILAR CONDITIONS

by

Ülar Tiitma

A Thesis

Submitted to the
Mechanical Engineering
College of Engineering
In partial fulfillment of the requirement
For the degree of
Master of Science in Mechanical Engineering
at
Rowan University
May 30, 2024

Thesis Chair: Francis M. Haas, Ph.D., Associate Professor, Department of Mechanical Engineering

Committee Members:
Joseph F. Stanzione, III, Ph.D., Professor, Department of Chemical Engineering
Behrad Koohbor, Ph.D., Assistant Professor, Department of Mechanical Engineering

Acknowledgments

I would like to express my appreciation to Professor Francis M. Haas, Ph.D., for his continuous encouragement, expert advice, and dedicated mentorship, which have been instrumental in guiding me through this academic journey.

I would like to thank Tristan W. Bacha and David A. Brennan, whose collaboration at the inception of this project and their invaluable assistance were instrumental in understanding and developing the complexities of the polymer cold spray.

Abstract

Ülar Tiitma
STUDY OF POLYMER-ON-POLYMER COLD SPRAY DEPOSITION WINDOWS UNDER APPARENTLY SIMILAR CONDITIONS
2023-2024
Francis M. Haas, Ph.D.
Master of Science in Mechanical Engineering

The purpose of this thesis is to explore and expand the capabilities of polymer-on-polymer cold spray demonstrated herein using polyamide 6 (PA6)-based powder and substrates. Experiments were conducted using three different cold spray systems described in this work, permitting more in-depth examination of process response to different cold spray process control parameters, such as nominal system pressure and temperature. Two specific responses of interest were the deposition window (DW) and deposition efficiency (DE) of PA6. The DW was determined by performing several sprays at different calculated particle impact velocities and temperatures. The composite result from these experiments was identification of a large DW in which the role of the particle impact temperature was noticeable enough that, in addition to critical velocity, present results suggest that a critical particle temperature should be considered when determining DWs for polymer powder spraying. Additionally, the combined DW results from all three systems show that particle impact velocity and particle impact temperature alone may be too simple to describe clear regions of deposition. The DE was determined by using a single low-pressure, downstream injection cold spray system. Under favorable conditions, a DE of ~67% was measured for PA6, roughly seven times higher than the highest DE previously described in the literature for polymer-on-polymer cold spray.

Table of Contents

Table of Contents (Continued)

Table of Contents (Continued)

List of Figures

List of Figures (Continued)

Figure Page

List of Tables

Table Page

Chapter 1

Introduction

Within the past 100 years, humankind has come a long way from the Ford Model T to the Tesla Model S. The technological advancements over that time have been remarkable. To accompany all-new innovations, there is also a need for new manufacturing techniques. With the advent of 3D printing, the field of additive manufacturing has steadily become more prevalent in the field of manufacturing. One of the newer technologies included under the umbrella of additive manufacturing is cold spray processing, also commonly known as cold gas dynamic spray or just "cold spray".

Cold spray is a process of applying coatings to the substrates by a high velocity (~300 – 1500 m/s) jet of small particles (~5 – 100μm) [1]. Most commonly, powder particles are accelerated by a gas stream through a DeLaval type nozzle to supersonic speeds. The gas temperature is always kept below the melting point of the material being sprayed (hence, the process is "cold" compared to the melting temperature). For metal powder, high-velocity impact results in particles being plastically deformed, creating a combination of metallurgical and mechanical bonding with the surrounding material in a solid-state [2]. The bonding mechanism(s) for polymers may differ, which work in this thesis seeks to explore further.

The fact that there is no initial phase change in the material being sprayed often minimizes or eliminates problems such as high-temperature oxidation, evaporation, melting, crystallization, residual tensile stresses, debonding, and gas release, among other

commonly encountered problems. By avoiding those problems, cold spray can offer significant advantages and new possibilities for many industrial applications. [3]

The cold spray process was first developed in the mid-1980s by the Institute of Theoretical and Applied Mechanics of the Russian Academy of Sciences [3]. Since then, the technology has rapidly developed, and it is currently primarily used for repairing and creating new surface coatings, but it is also possible to create near-net-shape parts similar to other additive manufacturing processes [2]. The most significant advantage of cold spray is that it is a solid-state process, which results in many desirable characteristics such as high deposition efficiency and rate, high density, and reduced thermal input to the substrate [4]. The most significant limitation is the loss of ductility, especially without any post-spray treatment [4].

Everything mentioned above has one caveat: most of the work done on cold spray technology over the past 30 years has involved metals and metallic composites [2]. Advances in the materials sector and applications of new materials/processing have come a long way since the 1980s, and there are a lot of new materials worth exploring with cold spray [5]. One class of these materials are polymers. These have been studied for cold spray application [6-10], but not to the extent that metals or ceramics have [5]. This thesis explores the current state and practical feasibility of polymer cold spray, particularly for the thermoplastic polymer polyamide 6 (PA6), also known as nylon 6.

1.1 Physics of Cold Spray

Cold spray involves spraying fine-size particles (few to tens of microns) at high velocities onto a substrate where the coating is produced through complex deformation and bonding mechanisms [2]. In order to achieve coating on the substrate, multiple spray parameters need to be considered. Broadly, those parameters could be grouped as propellant gas, feedstock material, substrate, and spray setup [2]. A basic setup (though not the only one) for cold spray processing can be seen in Figure 1. This simplified schematic gives a good general overview of the cold spray system.

Figure 1

Configuration of a Typical Cold Spray System

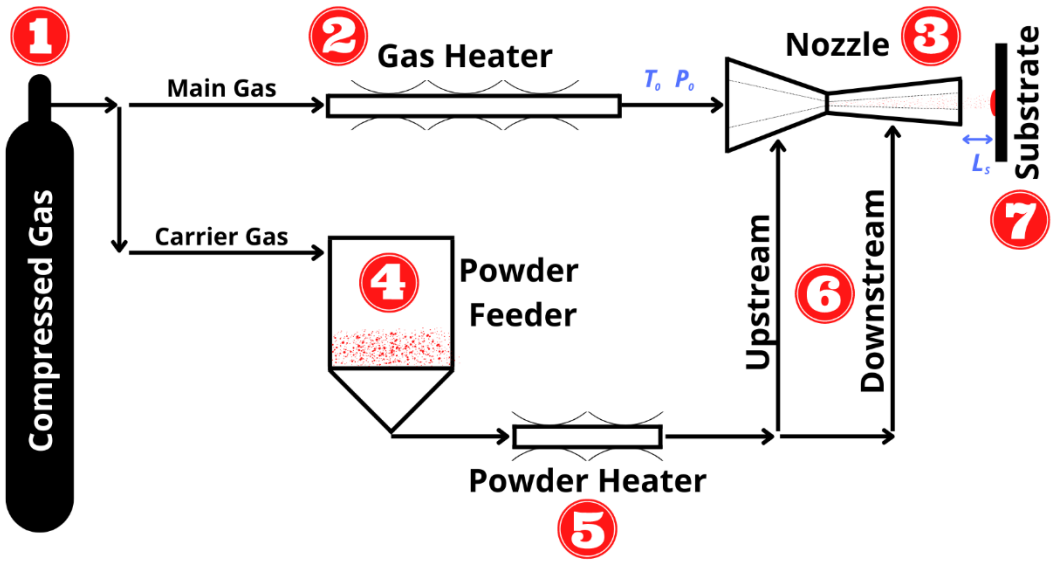

When dealing with propellant gas, the nature of gas, the gas stagnation pressure (P_0), and temperature (T_0) should be considered when choosing between different types of gases [2]. Most commonly, helium and nitrogen are used as propellant gas in a cold spray system, but compressed air is also used, which can cut down the cost of gas.

The feedstock material is the powder that is being sprayed. The parameters that need to be considered when cold spraying are the different characteristics of the selected powder, such as composition, particle size, size distribution and geometry, particle feed rate, and particle impact temperature [2].

The substrate is the surface onto which the powder is being sprayed. The parameters that need to be considered when cold spraying are the material of the substrate compared to the powder (similar or dissimilar materials), surface preparation before spraying, and substrate temperature [2].

After selecting the powder and substrate materials and the proper propellant gas, the cold spray unit must be set up correctly. The parameters affecting the successful spraying with the units are nozzle geometry and material, traverse speed, orientation, and distance from the substrate (stand-off distance, L_S) [2].

The end goal of cold spray is a successful deposition, but that is dictated by a large number of process parameters mentioned above. What makes controlling those parameters even more challenging is that some of them are interrelated [2], requiring further investigation to better illustrate how those parameters are interrelated. The

following subsections will describe the essential functions of those parameters mentioned above.

1.1.1 Cold Spray Process Description

The cold spray process starts with a reservoir of high-pressure compressed gas (Figure 1, item 1) that is usually divided into two streams: the main or process gas and the powder carrier gas [1]. For both of those gas streams, there are several controls to regulate flow rate, pressure, and temperature. The main gas is usually directed through an electric inline gas heater (Figure 1, item 2) into some type of applicator or spray gun (Figure 1, item 3) that includes some type of a nozzle. The reason for heating the main gas is not necessarily to heat or soften the spray particles but instead to achieve higher gas velocities [11]. The carrier gas is first directed through a powder feeder (Figure 1, item 4), inside which it picks up the powder, and after which it meets up with the main gas in the applicator/spray gun. The carrier gas is sometimes heated (Figure 1, item 5) to soften or heat powder particles before reaching the applicator or spray gun [2]. Chapters 3 and 4 further discuss (pre)heating of the powder.

The powder that is fed to the carrier gas is usually controlled by a specific feed mechanism (i.e., the powder feeder – usually based on rotary drum, brush sieve, or fluidized bed powder feed mechanisms) [1]. A specific flow rate of particles must be introduced to the carrier gas to achieve smooth, controlled spraying [1]. Usually, there are two types of powder injection methods - upstream and downstream (Figure 1, item 6) [1, 2]. The carrier gas is heated and mixed with the main gas in the applicator. It flows through a nozzle (Figure 1, item 3), often of the converging-diverging (de Laval) type [1,

2], which can accelerate gas flows to supersonic velocities. The gas expands within and beyond the nozzle, and the particles accelerate due to the drag force exerted on the particles by the expanding gas [1, 2]. Usually, gas expansion leads to particle velocities from several hundred to over one thousand meters per second. Particles are aimed at a substrate (Figure 1, item 7) that is often situated 10 - 50 mm from the end of the nozzle [1]. If the particles have acquired sufficient kinetic energy and possess suitable material properties, they can deform plastically and adhere to the substrate, but not all particles have enough kinetic energy to adhere to the substrate [1, 2]. The amount of powder particles adhering to the substrate compared to the amount used from the powder feeder is defined as deposition efficiency, as discussed further below. The entire cold spraying process can be noisy and dusty, typically requiring a spray booth for noise and fugitive powder control [1].

1.1.2 Process Gas

An example schematic for cold spray can be seen in Figure 1. This differs from machine to machine, but the main components are the same. Compressed gas (sometimes called process, propellant, or main gas), which typically is helium (*He*), nitrogen (N_2), air [2], or a mixture of those gases (e.g. [12, 13]) and a patent exists for hydrogen (H_2) propellant [14]. Helium and nitrogen have an advantage for spraying metals and other oxygen-sensitive powders because they are inert gases [2]. Also, lower molecular weight gases such as helium are especially useful because they can reach higher velocities as they expand through a specific nozzle geometry [2], thereby dragging particles to higher velocities. While this suggests that helium is the best option for the main gas used in cold

spray, the cost of helium can be a limiting factor [2]. For this reason, nitrogen or air might be a preferable choice. For the case of air, in certain applications, a simple portable compressor can be used as the main gas supply source; however, this depends on the application's pressure requirements, and the fact that air is not an inert gas can be a problem with certain materials.

In some applications, helium and nitrogen mixtures are used as the main gas. One advantage of mixtures is that they yield improved heat transfer into the spray particles [12]. Compared to a pure light gas, using a gas mixture affects the velocity of gas (and, therefore, sprayed particles) because of the heavier molecular weight of the blend, which can result in coatings with reduced density and hardness [12]. This may be acceptable for some applications, which can benefit from reduced cost of gas propellant [13].

1.1.3 Powder Injection Types

In Figure 1, two powder injection types are shown: upstream and downstream. There are distinct differences between the two injection types that require a deeper dive, as discussed below. The cold spray units described in Chapter 2 use both powder injection types, providing an excellent practical example of how they each work.

The upstream injection configuration is when the carrier gas with powder is introduced to the applicator or spray gun before the nozzle's throat, as shown in Figure 2. This setup requires a robust pressurized powder feed system because of the high local pressure at the injection point of the particles [1].

Figure 2

Upstream Injection System

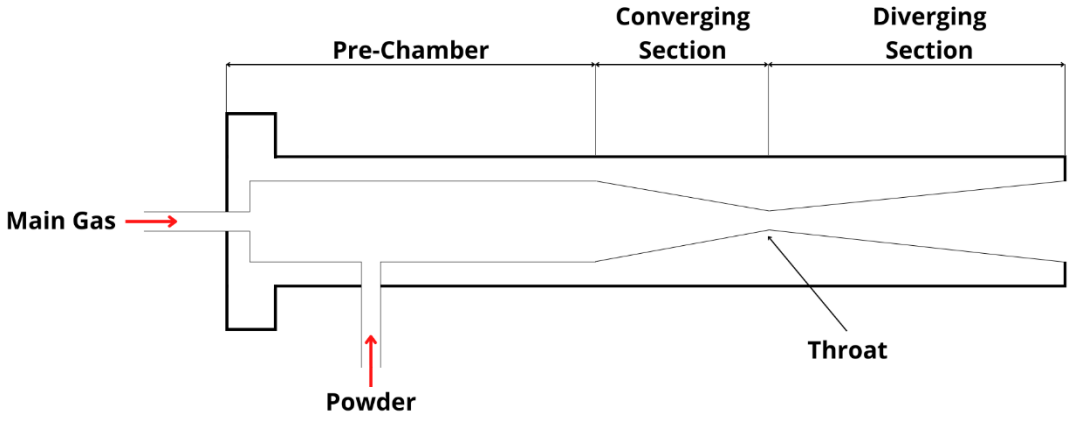

The alternative option is the downstream injection powder feed configuration shown in Figure 3. This is when the powder is introduced after the nozzle throat. At this point, the pressure is lower than the local pressure at the injection point [1]. In many cases, the pressure in the throat is below ambient atmospheric pressure, meaning no complicated pressurized powder feed system is required because the atmospheric pressure drives the carrier gas flow [1].

Figure 3

Downstream Injection System

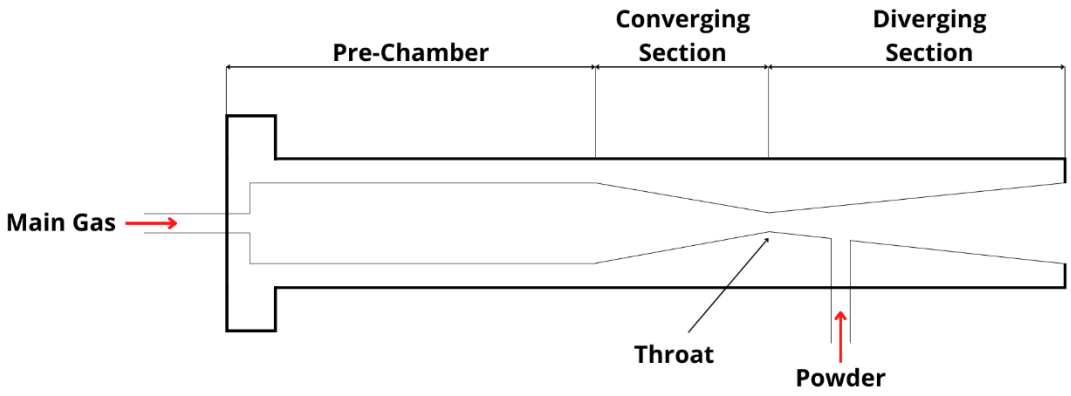

Usually, an upstream injection configuration is used in a high-pressure cold spray system (particle velocity ~200 to 1200 m/s or system pressure maximum of 40 bar), while downstream injection is used in a low-pressure system (particle velocity ~350 to 700 m/s or system pressure maximum of 10 bar) [15]. Comparative studies of copper powder cold spray have shown that high-pressure systems produce a denser deposition compared to low-pressure systems [15]. One important thing to note is that higher main and carrier gas pressures do not automatically mean higher particle velocity. The particle impact velocity and temperature depend on many variables - the temperature of the main gas, the pressure of the main gas, the nozzle geometry, and the powder, among others [1]. Chapter 4 presents an example of this.

1.1.4 Nozzle Design

The nozzle is the final and perhaps the most important part of the cold spray hardware. Its purpose is to convert the kinetic and potential energy of the gas into kinetic

and thermal energy in the particles, direct the particles towards the substrate, and control the deposit size [1]. The aforementioned paragraphs only mentioned a supersonic nozzle (converging-diverging), but a sonic nozzle can also be used in cold spray. Both types of nozzles have similar converging sections followed by a throat, which has the smallest cross-sectional area for the flow, where the flow reaches the speed of sound (gas is sonic) [1] if a specific minimum pressure ratio across the nozzle is provided. Beyond the throat, the geometry of the diverging section determines how much the gas expands and reaches supersonic speeds (supersonic nozzle) or maintains the sonic speed (sonic nozzle) [1]. Because of the significant area expansion downstream of the throat, the nozzle geometries indicated in Figure 2 and Figure 3 are both supersonic regardless of their powder injection type. The sonic nozzle shown in Figure 4 has a slight divergence, where the boundary layer formed in the diverging section maintains a constant effective diameter (i.e., no effective divergence).

Figure 4

Sonic Nozzle Geometry

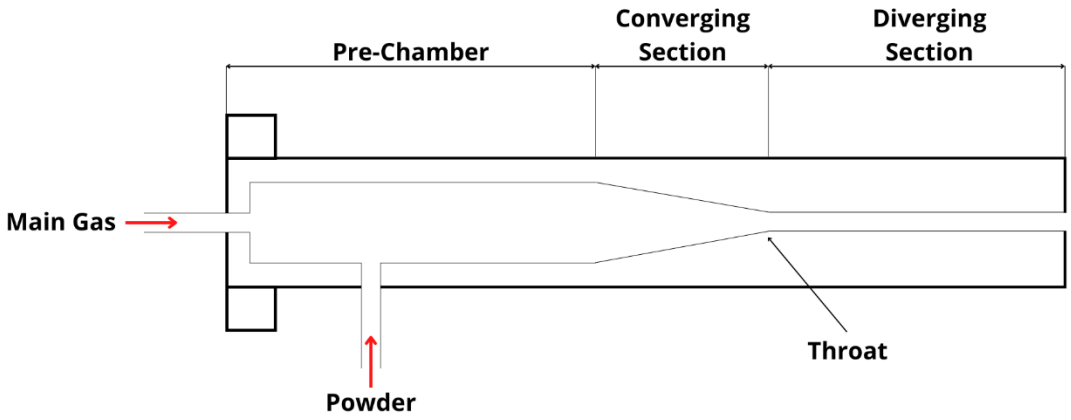

Gas expansion in the diverging section leads to an increased particle kinetic energy, which can be good under some circumstances, but this is done at the expense of gas enthalpy and, therefore, pressure and temperature [2]. The gas temperature drop can be significant, which typically means the particle temperature remains below the melting point of the particle material. That is what makes cold spray unique compared to other thermal spray systems, but in some instances, the particle temperature can drop too much [2]. Too low of a particle temperature could affect material ductility, which in turn could decrease the particle's ability to deform upon impact with the substrate and create a successful deposition [2]. This is where powder preheating might be beneficial in counteracting the large temperature drop in the diverging section of the nozzle [2]. Another option to avoid particle cooling would be to use a sonic nozzle, where gas expansion is limited, and a large temperature drop can be avoided. However, this is at the expense of the gas velocity. This is why both sonic and supersonic nozzles are used in cold spray systems, as further discussed in Chapters 3 and 4, where this problem was tackled experimentally.

One more factor to be considered for gas expansion in the diverging section is gas density, which is important because it affects how well the gas flow can accelerate particles through the nozzle. After all, the drag force (F_d) on a representative particle is proportional to the gas density (ρ_g) and the square of the relative velocity between the particle and the gas:

$$F_d = \frac{C_d A_p \rho_g \left(V_g - V_p\right)^2}{2} \tag{1}$$

C_d is the particle drag coefficient, A_p is the effective particle area, V_p is the particle velocity, and V_g is the gas velocity. Suppose the gas density falls significantly, as can happen in the nozzle designed for extremely high Mach number (thus, gas velocity). In that case, the gains made by increased velocity are reduced by the density drop [2]. For all the reasons mentioned above, cold spray nozzle design Mach numbers are usually kept below Mach 5 (below the hypersonic speeds) [2].

1.1.5 Critical Velocity

The previous paragraph outlined why trying to achieve high gas velocities (high kinetic energy) might not be the best idea. However, particles must have enough kinetic energy to plastically deform and adhere to the substrate. In other words, the gas needs to accelerate powder particles up to a certain velocity. The minimum required particle velocity under which the particles successfully adhere to the substrate is called critical velocity (V_{crit}) [1, 2]. Below the critical velocity, the substrate is eroded by a stream of particles (similar to sand blasting).

The critical velocity is not a fixed number; it changes as particle temperature changes [1]. Additionally, not all the particles in a powder are of the same size, which in turn can lead to different velocities and temperatures of the individual particles in each batch [1], as will be discussed further in the next chapter. All the variabilities make predicting the critical velocity difficult, but it can be done either by measuring it experimentally or predicting it by numerical modeling [2]. At least for metals, one way to estimate V_{crit} is through empirical particle material properties relationships between the ultimate tensile strength (σ_u) measured in MPa at room temperature, the density (ρ) in

g/cm^3, melting temperature (T_m) in ^{o}C, and impact temperature (T_i) of the powder in ^{o}C. The critical velocity can be found through Equation 2 [16]:

$$V_{crit} = 667 - 14\rho + 0.08T_m + 0.1\sigma_u - 0.4T_i \quad (2)$$

Even though Equation 2 is only valid over a limited range of material properties and process conditions, it gives a good overview of how the material properties affect the critical velocity [16]. One thing to keep in mind is that bulk material properties might differ from micron-sized particles of the same material [17].

The critical velocity is a useful tool to determine the minimum velocity for which the deposition of particles is possible. However, to have a dense, high-quality coating, impact velocity needs to be at least 150% of V_{crit} or even higher [1]. That is where optimizing the spray conditions comes into play, which is beyond the scope of this thesis.

1.1.6 Powder

In the literature, a wide range of powders have been used in a cold spray, generally metals-on-metal alloys, composites, or polymer powders [1]. Polymer cold spray is the main focus of this thesis. Still, because a majority of research into cold spray has been done with metal or its composite powders, the examples discussed below will involve those types of powders. Regardless of the material, the general understanding of the importance of the feedstock material remains the same. Some of the important properties of the feedstock powders to consider are hardness, ductility, particle size, morphology, thermal properties, flowability, electrical conductivity, etc. [1, 2]. The powder's ductility and hardness directly affect how successfully the powder particles

adhere to the substrate because the particles have to plastically deform to adhere to the substrate [1, 2].

Another factor that will be mentioned throughout Chapters 3 and 4 is the particle size and morphology. The size of the cold spray powder particle generally stays between 5 – 100 μm [2]. Particle size varies in a single powder batch, so powder is often defined by an average effective powder diameter and a size distribution. Cold spray usually requires narrow powder size distribution; the most commonly used ranges are 5 – 25 and 15 – 45 μm. The need for narrow distribution is because the particles of different sizes will each have a different critical velocity, which directly affects the deposition of the powder [17]. The rule of thumb is that the smaller particles achieve higher velocities [2]. This would suggest that the smaller the particles, the better the chances for their successful deposition. However, there is also a lower limit for particle size because of the bow shock effect, which will be explained more in Chapter 3. It has been shown that the deposition efficiency drop has been significant, from 90% at 8 μm to 50% at 2 μm [18].

In addition to the size of the particle, the shape of the particles (morphology) is an important factor to consider. Typically, the particle can be spherical, elongated, or blocky [1]. In the literature, it has been shown with pure titanium that the medium-sized spherical particles (average 29 μm) have the best sprayability based on the deposition efficiency, critical velocity, and porosity [19]. This is only one specific powder in a specific cold spray device, and in reality, each cold spray requires a particular size of powder distribution based on its design [17, 20]. The particle size and the morphology

together determine the free surface area per volume, where the large surface area can result in degraded coating quality [17].

1.1.7 Substrate

As mentioned above, the particle must achieve a certain critical velocity to undergo sufficient plastic deformation to adhere to a substrate. Thus far, deposition has only been discussed in terms of the particle, but successful deposition also depends on the characteristics of the substrate because adhesion strength is a combination of particle deceleration and the distribution of energy dissipation in the particle and substrate [17]. At the same time, it has been shown that the substrate's hardness affects the deformation only when the formed coating is thin [21].

There are also ways to influence the deposition by the temperature and the surface roughness of the substrate. In the literature, it has been shown with aluminum, zinc, and tin powders that heating the substrate has an effect on deposition efficiency [22]. Something to keep in mind here is that the surface temperature is not the same as the overall temperature of the substrate. The surface temperature is also affected by such factors as spraying conditions, thermal properties, and spraying kinematics [17, 22]. The surface roughness and the presence of oxides and surface contaminants can also affect the spray's bond and quality [1]. Surface roughness can be changed by blasting or machining, and the oxide layer can be removed by blasting or sanding [1]. It has been shown that grit blasting a surface increases the deposition efficiency, but it can also lower the bond strength of the spray [23, 24].

1.1.8 Deposition Efficiency

In the subsection above, most of the cold spray parameters affecting deposition have been introduced. The end goal of cold spray is to achieve a successful deposition with high quality, though "success" and "quality" are subjective terms. One of the simplest objective ways to determine spray success is by measuring deposition efficiency, which is a telling parameter because, usually, not all particles successfully deposit onto a substrate. Particles that fail to deposit tend to rebound or splash off the surface.

The deposition efficiency (*DE*) is the ratio of the mass of powder deposited onto the substrate to the total mass of the powder sprayed [2]. It is usually presented as a percentage and calculated by Equation 3 [2], where Δm is the sample's mass increase, and M_0 is the total mass of material fired at the sample. Finding the deposition efficiency is relatively straightforward and one of the most telling parameters of a successful spray. In the industry today, metal sprays can reach nearly 100% deposition efficiency under certain circumstances [25].

$$DE = \frac{\Delta m}{M_0} \tag{3}$$

Most of the examples and literature citations throughout this chapter were about metal cold spray, but as mentioned in the beginning, this thesis is about polymer cold spray. Over the past ~37 years, metal cold spray has seen substantial advances, and it now has a significant potential in future manufacturing processes. Expanding its material variability is one way to make cold spray manufacturing even more feasible for

commercial use. From this point on, this thesis focuses almost exclusively on polymer cold spray. The end of this chapter summarizes the current state of polymer cold spray.

1.2 A Brief History of Polymer Cold Spray

The majority of both research and applied work with cold spray has been done with metal powders. However, metals have their limitations, and in recent decades, the polymeric components used in aircraft, automobile, and power sectors have increased because of the need for weight-saving [26]. This is why research into polymer cold spray is now more relevant than ever. In general, polymers can be classified as thermoplastics (such as poly(methylmethacrylate) and polyamide (PMMA and PA, respectively)), thermosets such as epoxy, and elastomers such as natural rubber [27]. Some types of polymers, such as polyimide and polyurethane (PI and PUR, respectively), may fall into more than one category depending on specific material chemistry.

Spraying polymer by itself has its problems, as will be mentioned throughout this thesis, and one way to avoid some of them is to combine metal and polymer. One technique is surface metallization, where the polymer substrate is covered with metal through cold spraying (metal-on-polymer cold spray). This helps to enhance erosion resistance and address poor thermal/electrical conductivity of the substrate [28]. The literature has multiple examples of using cold spray for surface metallization [26-28]. This particular application is enticing because of the lower heat input of cold spray compared to other thermal spray coating techniques. The reduced heat input reduces surface distortion, oxides, voids, phase transformation, and residual stresses in the coatings [28].

The opposite combination of spraying polymer powder onto a metal substrate has also been performed with varying success [7, 29]. Studies of cold spray of polymer powder onto the metal substrate (polymer-on-metal cold spray) seem to indicate that a thin initial melted polymer layer needs to be applied onto the metal substrate [7] or higher particle temperatures and lower particle velocities are necessary for a successful deposition [29].

Polymer powder being sprayed onto a polymer substrate (polymer-on-polymer cold spray) is a third option for how polymers can be used in a cold spray, but significantly less literature is available for this compared to cold spray processing involving metals. Prior to the writing of this thesis, some of the few published examples of polymer-on-polymer cold spray included polyolefin powder onto high-density polyethylene (HDPE) substrate [7]; HDPE powder onto HDPE, polyvinylchloride (PVC), polyoxymethylene (POM), and low-density polyethylene (LDPE) substrates [6]; HDPE, polyurethane (PUR), polyamide-12 (PA12), polystyrene (PS) and ultra-high molecular weight polyethylene (UHMWPE) powders onto HDPE, PVC, POM, and LDPE substrates [8]; and ultra-high molecular weight polyethylene (UHMWPE) powder onto polypropylene (PP) substrate [30]. These polymer-on-polymer spray results have shown that polymer particles do behave significantly differently from metal particles during the spray because of differences in mechanical properties, elastic modulus, thermal conductivity, degree of crystallinity, and (in)availability of metallic bonds [6, 7]; however, these studies are still not sufficient to permit facile manufacturing “recipes” for polymer cold spray applications that permit prediction of final material properties based on the initial

material structure/properties and processing conditions. This is the reason why more research needs to go into polymer cold spray.

As mentioned, successful polymer-on-polymer cold spray experiments have shown potential in polymer cold spray. One of the most important metrics for success in cold spray is the deposition efficiency. In this metric, polymer cold spray lags far behind metal cold spray. In the experiments mentioned above, Xu et al. [7] were able to spray polyolefin onto HDPE substrates with a deposition efficiency of <0.5% in one of the first documented polymer spray studies, while Bush et al. [6] were able to spray HDPE powder onto LDPE substrates with a deposition efficiency close to 10%. The results of Xu et al. were published in 2006, while those of Bush et al. were published in 2017. This shows there have been substantial improvements in polymer-on-polymer cold spray deposition efficiencies. However, they are still far behind the nearly 100% deposition efficiencies that metal cold spray can reach.

Deposition efficiency is not the only important metric when considering cold spray. One of the more interesting discoveries made in polymer-on-polymer cold spray was from Khalkhali et al. [8]. They used a similar setup as did Bush et al. but considered more different polymer powder and polymer substrate combinations. The highest reported deposition efficiency was close to 10%, as was noted before. They also measured the mechanical properties of those samples, and it was concluded that the mechanical properties were roughly the same for the cold-sprayed samples as they were for the corresponding melt-cast specimens. That is an encouraging discovery, especially when considering using cold spray technology in 3D additive manufacturing [8].

1.3 Purpose of This Thesis

The overall goal of this thesis was to explore polymer cold spray capabilities further and improve upon current experimental techniques and hardware design. Specifically, this work seeks insight into determining conditions favorable for polymer particle deposition onto polymer substrates (i.e., finding the "deposition window"). Since polymers and polymer matrix composites continue to be of interest in manufactured goods, the unique aspects of polymer cold spray processing may open up many interesting manufacturing possibilities.

This thesis examines both cold spray hardware and, as will be shown, the *apparent* processing conditions for polymer cold spray. Some of the earliest polymer-on-polymer cold spray studies with extensive experimental data are from Bush et al. [6] and Khalkhali et al. [8], using the same cold spray unit. This specific cold spray unit was purposely built for polymer spraying, making it an attractive piece of hardware to replicate for the work described in this thesis and for more generally advancing polymer-on-polymer cold spray knowledge. Since this is a low-pressure system, it is relatively easy to use, and its particle velocities are quite low compared to cold metal sprays. Accordingly, a cold spray unit similar to that described in Bush et al. [6] and Khalkhali et al. [8] was built as part of the work for this thesis project. In addition, this thesis considers two different commercially purchased cold spray units that also permit spraying at *apparent* processing conditions similar to the Bush/Khalkhali device. A comparison of the performance of the three units allows for a deep dive into the specifics of a polymer-on-polymer cold spray, especially with respect to the deposition of particles.

The hardware and functional similarities/differences among all three cold spray units are described in Chapter 2. Chapters 3 and 4 focus on experiments with those three units under different spray conditions; more specifically, these chapters examine the deposition window of a polyamide 6 (PA6)-based polymer powder, the effects of preheating powder on deposition, and ways to increase the deposition efficiencies of polymer-on-polymer cold spray. Chapter 5 provides concluding remarks and offers suggestions for future work.

Work conducted as part of this thesis research is also described in the following publications:

T. Bacha, D. Brennan, **Ü. Tiitma**, F. Haas, and J. Stanzione, "Effects of Powder Feedstock Pre-Heating on Polymer Cold Spray Deposition," in ITSC2022, 2022: ASM International, pp. 44-55. doi: 10.31399/asm.cp.itsc2022p0044 [9], subsequently appearing with some modification in the *Journal of Thermal Spray Technology* vol. 32, no. 2, pp. 488–501, 2023, doi: 10.1007/s11666-023-01549-7

D. Brennan, T. Bacha, **Ü. Tiitma**, F. Haas, and J. Stanzione, "Systematic Study of the Effects of Powder Preconditioning on Flowability and Deposition in Polymer Cold Spray," in ITSC2022, 2022: ASM International, pp. 683-694. doi: 10.31399/asm.cp.itsc2022p0683 [10].

Chapter 2

Methods and Materials

2.1 Introduction

Determining suitable cold spray conditions using a capable cold spray unit is required to improve the current polymer cold spray results. As mentioned above, the differences in metal and polymer properties require different spray parameters (e.g., system pressure and temperature); this can be an issue when considering commercial units because many commercially available cold spray units have been developed for metal cold spray.

Considering this issue, a couple of important requirements for a polymer cold spray unit should be met. First, accurate temperature control of the main propellant gas at lower temperatures is necessary because polymers' melting point is comparatively low compared to metals. Secondly, thus far, polymer cold spray has shown relatively low critical velocity values, for example, 100 m/s for polyolefin powder [7], which is considerably lower than metal cold spray critical velocity, for example, 612 m/s for aluminum 6061-T6 [25]. Lower velocity requirements indicate that low-pressure cold spray units can be suitable for polymer spray.

Based on these considerations, three different cold spray units were acquired and used in this thesis. One of these was built in-house based on the cold spray unit design described by Bush et al. [6]. The other two were commercially purchased metal cold

spray systems from VRC Metal Systems [31] and BaltiCold Spray LTD [32]. The rest of this chapter focuses on the description and comparison of those units.

2.2 Benchtop Unit

The cold spray unit built in-house and based on the design of Bush et al. [6] is called the benchtop unit throughout the rest of this thesis. This was the very first working cold spray unit at Rowan University. From [6], the basic working principle and the exact nozzle dimensions were obtained, permitting a functional cold spray unit to be designed and built.

Its working principle can be seen in Figure 5. Based on system configuration characteristics described in Chapter 1, this unit can be defined as a low-pressure upstream injection cold spray - all functional components enclosed in a pressure vessel. The main gas (usually nitrogen or air) is heated before being pumped into the pressure vessel, inside which the vibrating hopper powder feeder is located. In this configuration, the main gas flow also heats the powder before it is sprayed (pre-heated powder). The powder feeder uses a simple vibratory feed mechanism, where one end of a rod is connected through a pressure seal to a pneumatic vibrator, and the other end attaches to a wire mesh inside the pressure vessel and at the base of the vibrating hopper. The nozzle is directly connected to the base of the pressure vessel.

The whole system works in the following way. The main gas runs from the gas source (i.e., compressor or gas tank) through an inline heater and into the pressure vessel. The gas heats the whole powder feeder and its contents inside the pressure vessel. The

powder is ejected from the feeder by vibrations of the wire mesh and gravity assistance, after which the main gas flow carries it through the nozzle to the target substrate.

Figure 5

Schematics of the Benchtop Unit (left) and Nozzle (right)

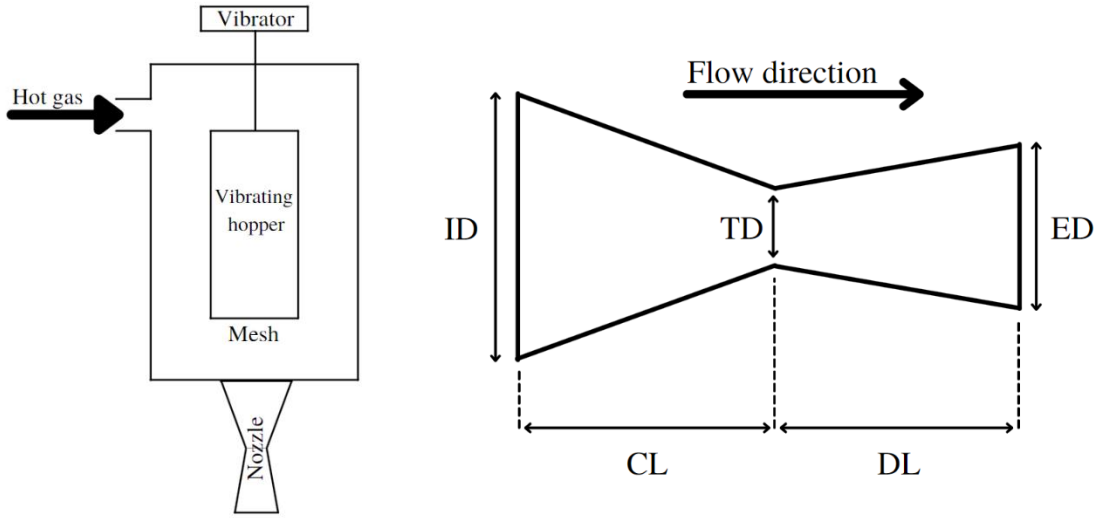

Note. Nozzle dimensions are described in the text.

The nozzle can be considered the most important part of the cold spray unit since its geometry regulates gas flow rate (and, therefore, heating requirements) and particle acceleration under normal operating conditions. Accordingly, selecting a specific geometry is important to achieve the particle temperatures and velocities required for successful cold spray deposition. Traditional nozzle materials such as tungsten carbide or polybenzimidazole (PBI) are specified to be compatible with the high temperatures and

high pressures of the main gas; however, as discussed below, polymer cold spray permits other nozzle material options.

The need for accurate dimensions can make the manufacturing process of the nozzle difficult, especially if done manually with a lathe or a mill. Also, little information is available regarding polymer cold spray and especially the exact dimensions of the nozzles used. Fortunately, Bush et al. [6] provided the exact dimensions of the nozzle they were using and a procedure for making them, thus facilitating nozzle fabrication for this thesis. The exact dimensions of the nozzle initially used with the benchtop unit are presented in Table 1, corresponding with the nozzle schematic in Figure 5. Ultimately, only a sonic nozzle option was made from the four different nozzle designs described by Bush et al. The reason for this was its production simplicity, especially when considering that the COVID-19 pandemic restricted laboratory and shop access.

Additional work with the benchtop unit revealed that effective nozzles for polymer cold spray can also be 3D printed by stereolithography apparatus (SLA) techniques. Specifically, a Formlabs Form 2 printer and a Formlabs High Temp V2 engineering resin were used to print nozzles that were useful at temperatures and pressures relevant to polymer cold spray conditions described in this thesis. While not the focus of this work, this is an important observation, particularly for polymer cold spray, because 3D printing could simplify nozzle production and geometry optimization.

Table 1

Dimensions of the Benchtop Unit's Cold Spray Nozzle

Nozzle	Inlet Diameter (ID), mm	Throat Diameter (TD), mm	Exit Diameter (ED), mm	Converging Length (CL), mm	Diverging Length (DL), mm
Subsonic nozzle	9.52	1.59	1.59	23.90	26.00

The first iteration of the benchtop cold spray unit can be seen in Figure 6. The pressure vessel was made of thin-walled stainless steel to avoid corrosion while providing enough strength to withstand an internal pressure of 100 psig (fixed by house air pressure limitations). The temperature rating was designed around a maximum value of 230 °C based on both the melting temperature of polymers like polyamide 6 (PA6) and polyamide 12 (PA12), which were planned to be sprayed, as well as the decomposition temperature of polytetrafluoroethylene (PTFE) tape used to seal some of the penetrations and fittings on the pressure vessel.

The reason for choosing the PA6- and PA12-based polymer powders was their commercial availability in nominal sizes below 100 µm. Commercial names for the PA6-based and PA12-based powders are BASF Ultrasint X028 [33] and Sinterit PA12 Smooth v2 [34]. The exact composition and list of ingredients of those powders are unknown, but they are optimized for laser sintering, which means they should also be a good option for cold spray applications because of the similarities between the two processes. These powders will be referred to as PA6 and PA12, respectively, throughout the rest of this

thesis. Based on particle size and size distribution, the mesh sizes for the vibratory feeder were selected to permit a good powder flow during mesh vibration. A 750 W inline heater with thermocouple-based PID control was used for heating the main gas, as this power rating was sufficient at all flow rates studied.

Additionally, band heaters were installed outside the pressure vessel to compensate for heat losses and maintain stable and uniform temperatures throughout the volume. Finally, the entire pressure vessel was wrapped in aramid insulation, as seen in Figure 6. The apparatus is inside a fume hood for health and safety reasons.

Figure 6

Photographs of the Benchtop Unit – First Iteration

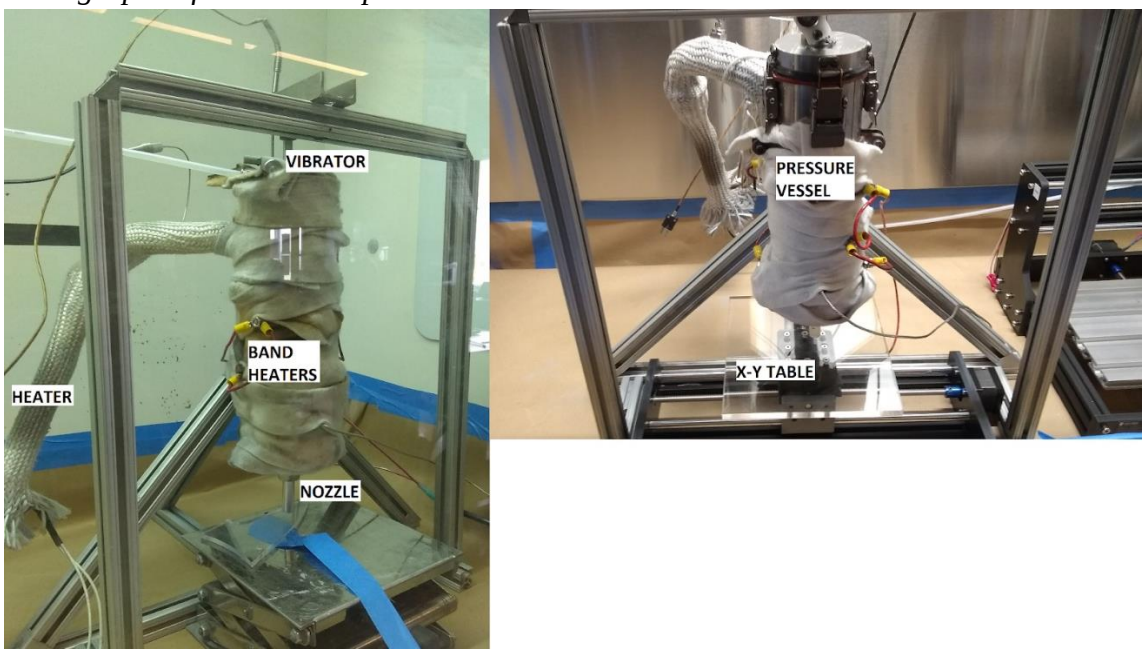

Initial testing with the first iteration of the benchtop unit was done without a proper X-Y translation stage, which limited controlled rastering of the spray plume. Instead, the cold spray jet was fixed for these tests, and the substrates were towed by hand. This approach worked for initial testing and showed that polymer powders can be sprayed with this unit.

However, after initial test sprays with this benchtop unit, a couple of problems with the first iteration design were identified. First, the lack of a proper X-Y table did not allow controlled traverse speed to enable scientific study (e.g., repeatability) of the cold spray process. Also, a need for z-axis motion was identified to maintain a constant offset (stand-off distance, L_s) between the nozzle and the substrate. These issues could be fixed by mounting the cold spray unit to a 3-axis CNC mill; however, the first iteration unit was too heavy for the CNC mill already in the lab. A second problem was that refilling the hopper with powder was time-consuming. The entire cap of the pressure vessel had to be removed to access the hopper for refilling, but this could not be done immediately after the spray session because the entire pressure vessel and hopper were hot. Both the weight/X-Y-Z positioning and hopper refill problems were addressed with a second iteration design discussed below. However, regardless of the difficulties posed by the first iteration of the benchtop unit, many proof-of-concept sprays were performed successfully. Some of the initial PA12 sprays onto the PMMA (acrylic) substrate can be seen in Figure 7. Those sprays used various pressure and temperature combinations, which are irrelevant to the present discussion.

Figure 7

Initial Benchtop Unit Spray Examples – PA12 onto Acrylic Substrate

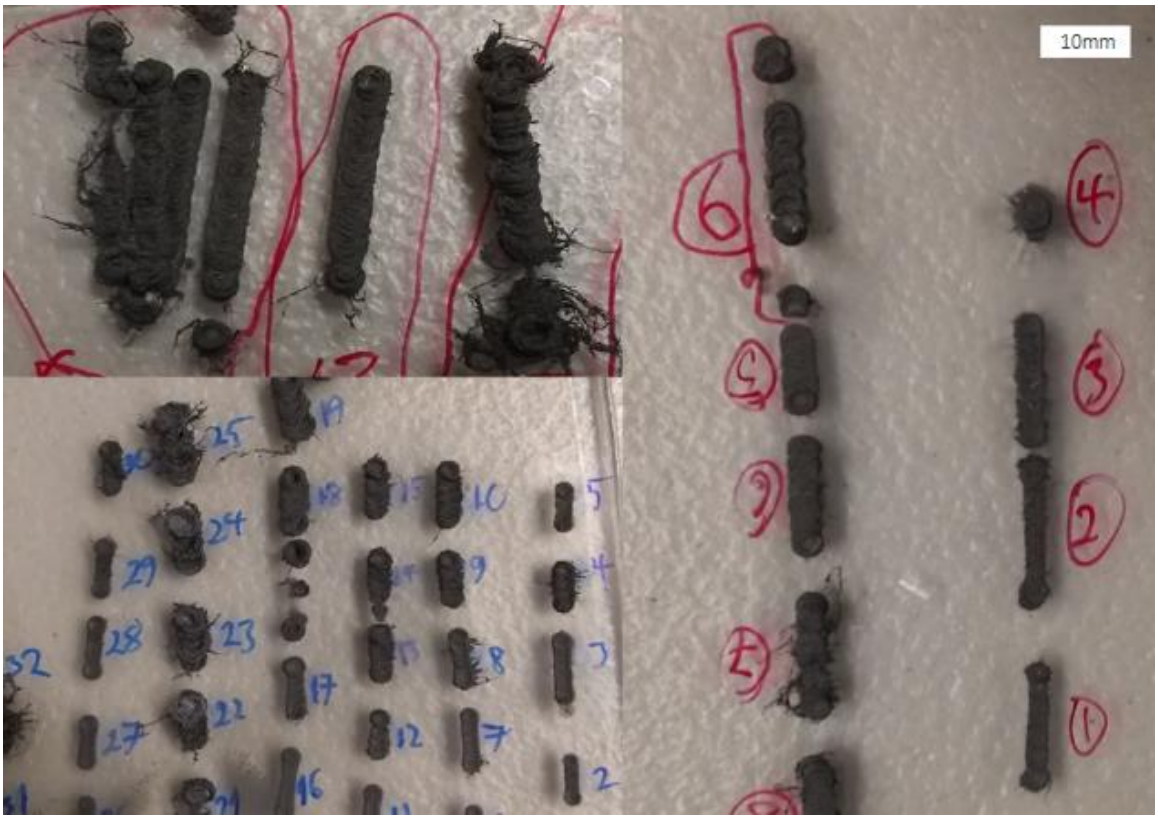

In order to perform more scientific studies and accomplish the deposition window measurements set for this thesis, the aforementioned problems with the benchtop unit had to be addressed. This involved updating the design of the pressure vessel and the hopper feed system. A new pressure vessel was designed out of aluminum to reduce weight (while maintaining mechanical strength), while the overall geometric parameters were kept the same. The hopper feed system was also redesigned by replacing the rod that connected the pneumatic vibrator with the mesh at the end of the hopper with a small metal tube that allowed nearly instantaneous refilling of the powder. Additionally, the

hopper walls inside the pressure vessel were thinned to speed up the heating of the powder during the initial heating transient. Though these improvements appear minor, preserving the overall principle and design of the benchtop unit, they enabled the second iteration to attach to a CNC mill and made system operation more user-friendly. A side-by-side comparison of the first and second iterations of the benchtop cold spray units can be seen in Figure 8. The control variables in those units are main gas pressure, main gas and powder temperature, feed rate of the powder feeder, and traverse speed of the CNC. Experiments conducted with this second iteration benchtop unit are described in Chapter 3.

Figure 8

Two Versions of the Benchtop Unit

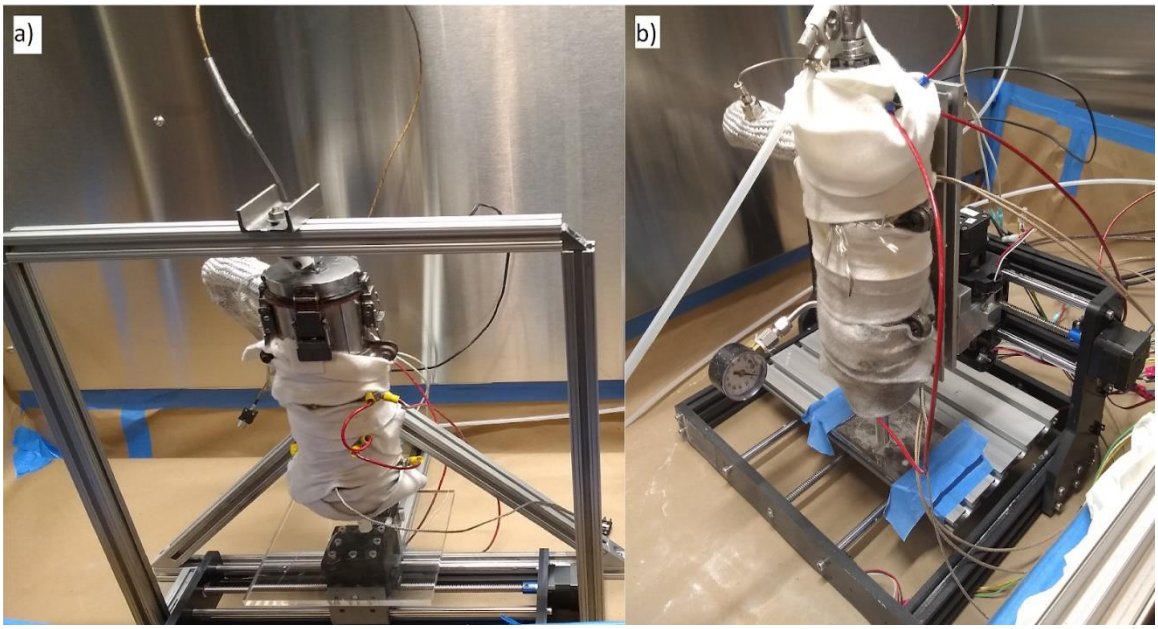

Note. The first iteration of the benchtop unit is picture a), and the second is picture b).

2.3 VRC Metal Systems Gen III Cold Spray System

As mentioned above, the two commercial cold spray systems were also used for the work described in this thesis. One was from VRC Metal Systems – The Gen III Cold Spray System. As the name suggests, this system was primarily designed for metal powders (e.g., alloys of magnesium, aluminum, copper, nickel, steel, and stainless steel). Still, based on the system operating parameters, it was assumed that this system could also be used for cold spray of polymer powders.

The main propellant gas for the Gen III system can be either nitrogen, helium, or a mixture of the two gases. The system can operate up to 1000 psi maximum pressure and 750 ^{o}C maximum temperature (measured at the applicator). This system has a stand-alone heater and a powder feeder converged in an applicator. The feeder needs to be pressurized because it has an upstream injection system, as described schematically in Figure 2. In the applicator, the heated main gas and the fluidized powder from the feeder are mixed and accelerated via a converging/diverging nozzle to deposit the particles onto a substrate. For the work described in this thesis, the feeder is not heated, which means the powder reaches the applicator at room temperature and has only moments to heat during the mixing phase. The applicator is connected to a 6-axis robot arm, allowing cold spray application along complex paths and geometries. Three different nozzles were used with this unit to widen the particle velocity and temperature window, as will be further described in Chapter 3. The primary process variables controlled for Gen III are main gas pressure, main gas temperature, feed rate of the powder feeder, gas flow rates, and traverse speed/path of the robot arm. The Gen III system is inside a spray enclosure,

which helps prevent dust accumulation and facilitates adherence to health and safety protocols. It is entirely controlled by a central human-machine interface (HMI), making repeatable experiments easy. The working principle of the Gen III cold spray unit can be seen in Figure 9, and the actual setup can be seen in Figure 10.

Figure 9

Working Principle of the VRC Gen III Cold Spray Unit

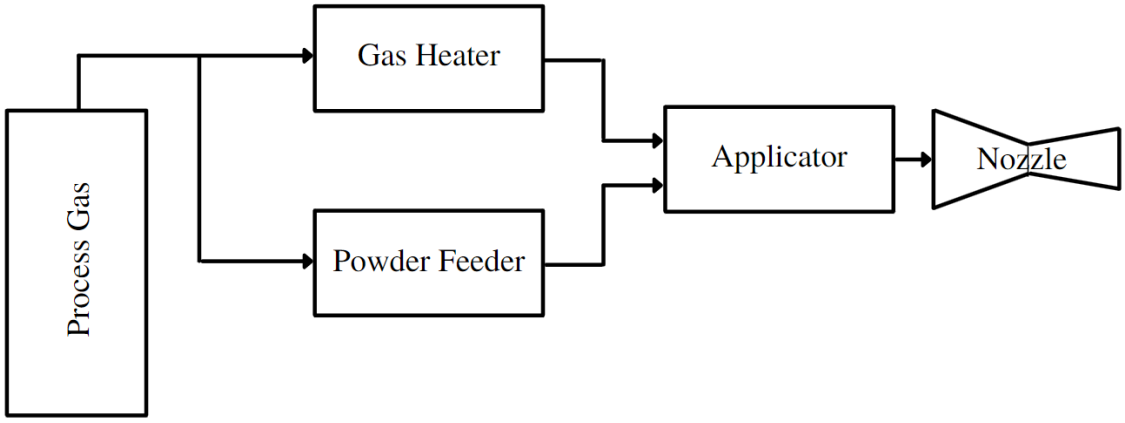

Figure 10

The Setup of the VRC Gen III Cold Spray Unit

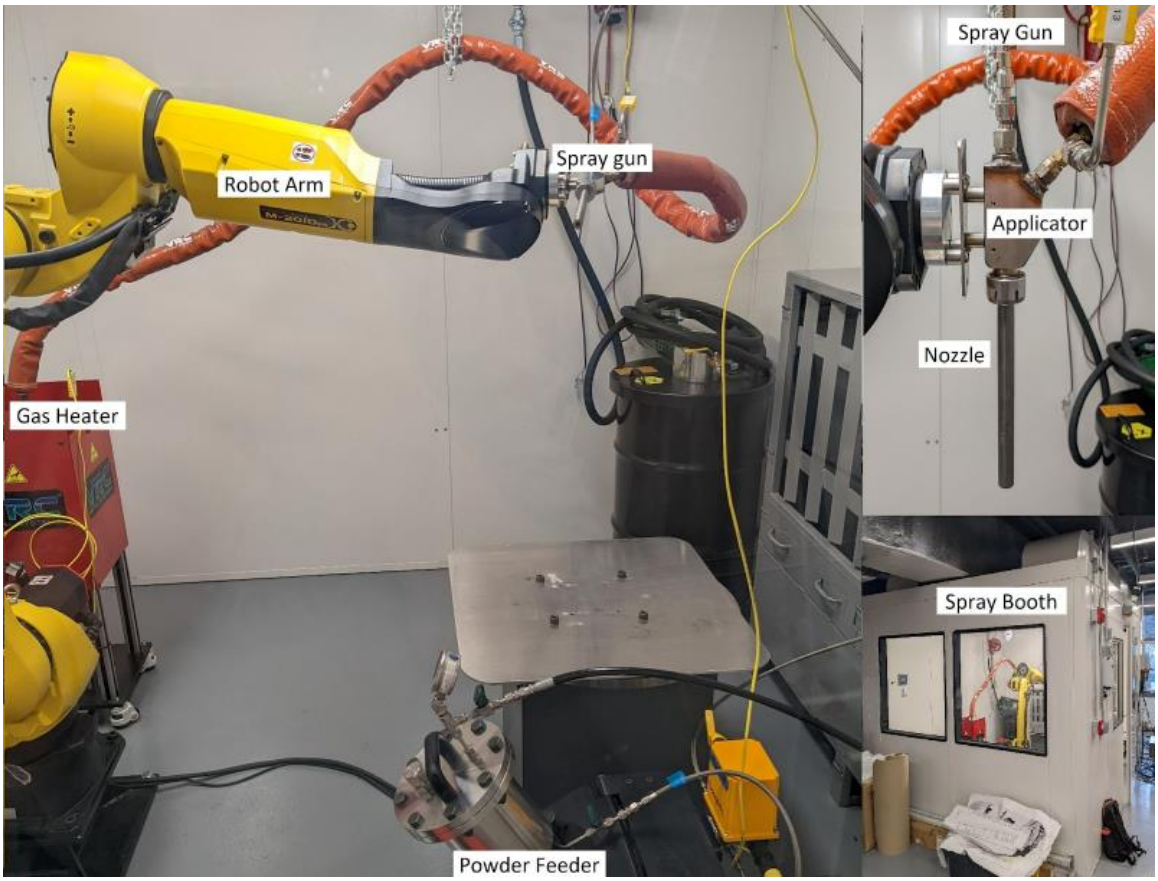

2.4 CSM 108 Portable Mobile Cold Gas Dynamic Spray Machine

The final cold spray used in this thesis is CSM 108, which was acquired from BaltiCold Spray LTD and based on a design from Dymet. It is a low-pressure downstream injection cold spray unit. This system is also meant for metal cold spray and, interestingly enough, sandblasting. Its operating pressure is between 90 and 170 PSI, and its maximum temperature is 600 ^{o}C. The fact that it is a low-pressure system permits using a compressor for a compressed gas source. This unit has a supersonic nozzle

directly connected to a heater, forming a handheld spray gun. Its downstream injection setup means there is no need for a pressurized powder feeder because the low pressure in the nozzle creates a suction that "pulls" in the powder, as described earlier in greater depth (Chapter 1.1.3). That configuration permits the CSM 108 to have a relatively simple vibratory powder feeder. The schematics of the unit can be seen in Figure 11.

Figure 11

Working Principle of the CSM 108 Cold Spray

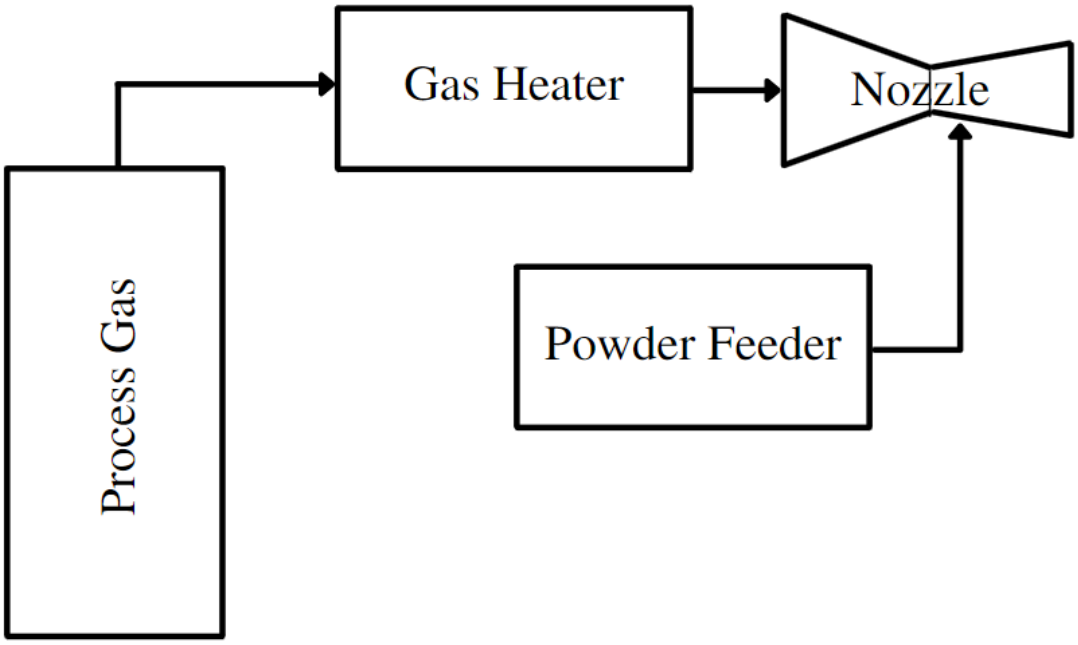

While the Gen III was also designed for metals, it came as a complete package ready for spraying. However, the CSM 108 required some modification before spraying polymers. To perform identical, repeatable sprays, the spray gun of the CSM 108 had to

be mounted onto some sort of robot arm or 3-axis table. Initially, the CSM 108 system used a similar CNC mill as was used with the benchtop unit, but eventually, a more advanced 3-axis table was built explicitly for CSM 108. In order to control the unit, the buttons on the spray gun had to be mounted onto a separate block outside of the fume hood where the 3-axis table with the spray gun was located. The original temperature control was without any feedback loop, which made knowing the exact temperature of the main gas difficult. The solution used for work in this thesis was to mount a K-type thermocouple between the spray gun and the nozzle, which allowed for accurate temperature control by an Arduino-based PID control system. The actual setup can be seen in Figure 12.

Figure 12

The Setup of the CSM 108 Cold Spray Unit

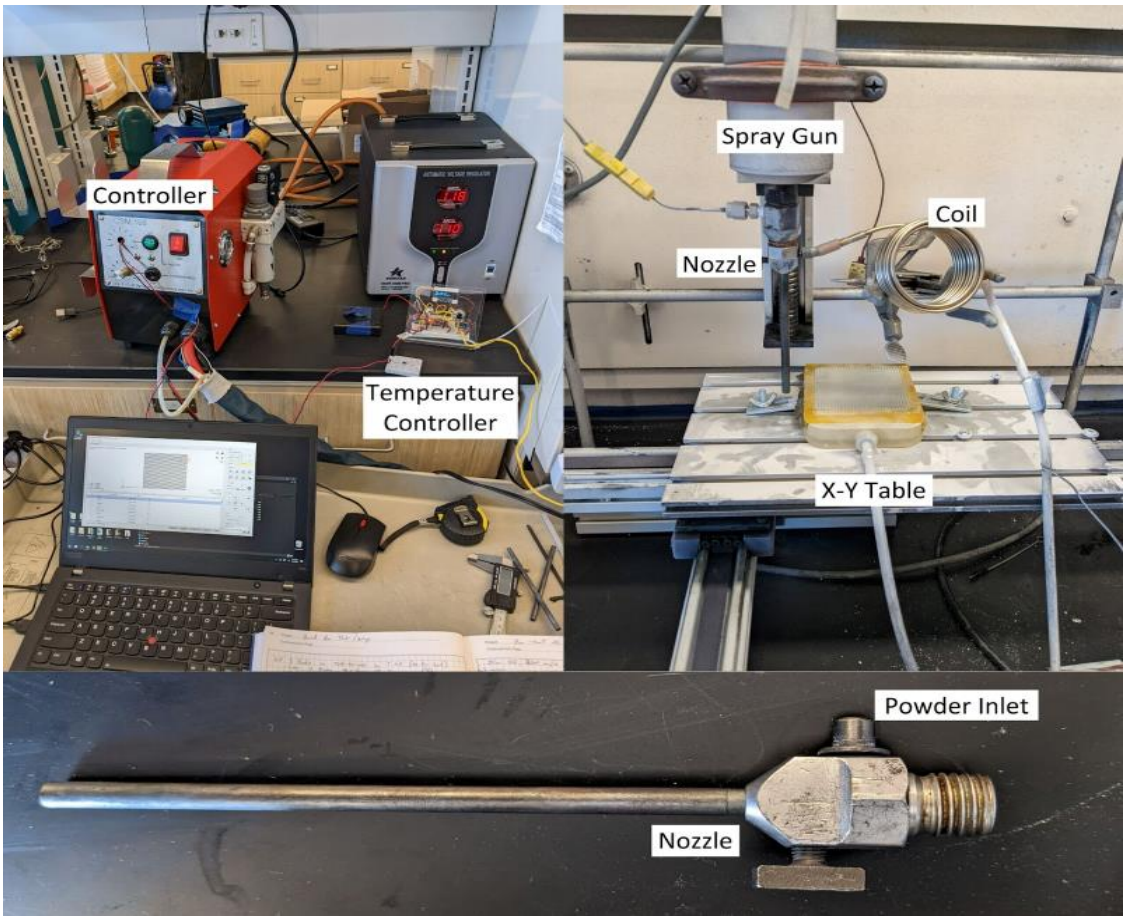

The previously described modifications allowed initial testing of the CSM 108 system, but in doing so, it was concluded that the original vibratory powder feeder could not provide a stable powder feed rate. Rather than trying to improve on the original, a different powder feeder was used. The downstream injection system simplifies the integration of the powder feeder. The new feeder design selected was based on the rotating drum design of The Gen III Cold Spray System [35], based on its simplicity and ease of control. This powder feeder has a drum with many small holes at the bottom. The

powder sits inside this drum, and all holes are filled as the drum rotates. The drum rotates over a base plate with a single hole connected to tubing, which leads to the nozzle. The rotation speed of this drum controls the powder feed rate.

One significant difference from the original Gen III powder feeder was that the new powder feeder for CSM 108 was entirely 3D printed. This was feasible because there was no need for pressurized powder feed, as mentioned earlier. The 3D-printed version of it can be seen in Figure 13. Having made the aforementioned improvements to the as-received CSM 108, the improved unit was ready to spray polymer powders. The process variables controlled in this unit include main gas pressure, main gas temperature, feed rate of the powder feeder, and traverse speed of the spray gun.

Figure 13

Powder Feeder for CSM 108

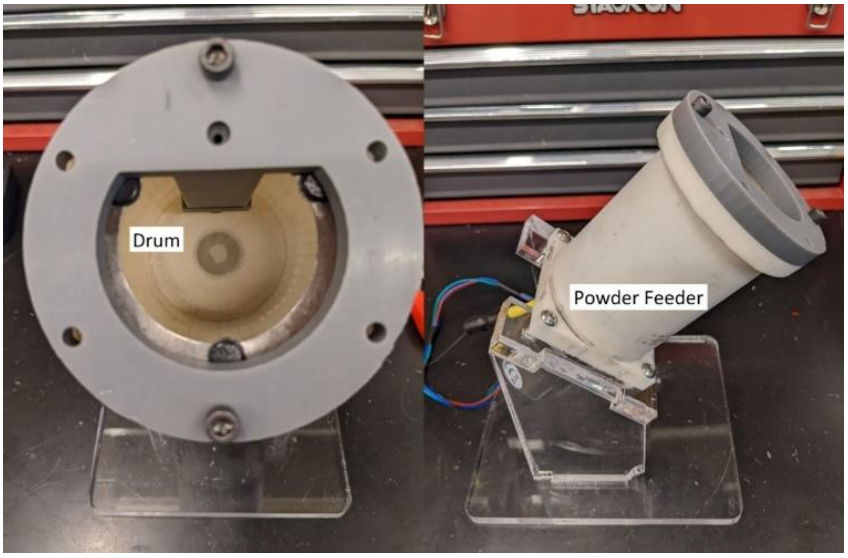

2.5 Comparison of the Cold Spray Units

Thus far, three different cold spray units have been described. To give a better overview of how they compare to each other, many of the important parameters of each cold spray unit are compiled below in Table 2. It is essential to have a good understanding of the capabilities of each of these units because all of them are used in experiments described in Chapters 3 and 4. As previously mentioned, only the second iteration of the benchtop unit was used in the experiments mentioned in Chapters 3 and 4.

Table 2

Comparison of the Cold Spray Units Used in This Thesis

	Benchtop unit	VRC Gen III	CSM 108
High/Low-pressure system	Low pressure	High pressure	Low pressure
Powder injection type	Upstream injection	Upstream injection	Downstream injection
Preheated powder feeder	Yes	No	No
Pressure range, bar	1.4 - 6.9	6.9 - 68.9	6 - 12
Maximum temperature, ^{o}C	230	750	600
Theoretical particle impact velocity range for PA6 at 100 ^{o}C, m/s (explained in Section 2.6)	141 - 207	246 - 431	379 - 409

As can be seen from Table 2, these three units cover most of the possible unit configuration combinations described in Chapter 1. This is important because there is not much experimental data on polymer cold spray, so these three units permitted experiments using different experimental setups to pinpoint the suitable settings for different polymer powders. The Gen III has the widest pressure range and highest pressure rating of the three. In order to reach those boundary pressures, various types of nozzles had to be used. That is why the calculated particle impact velocity range is also the widest for Gen III. The benchtop unit allowed testing of the lower end of the particle velocities where Bush et al. [6] and Xu et al. [7] had previously had success with different types of polymers.

Additionally, the benchtop unit preheats the powder, but the importance of this will be further discussed in Chapters 3 and 4. The CSM 108 is a low-pressure system that reaches roughly the same particle impact velocity as a more powerful Gen III unit. This characteristic appears in the discussion in Chapter 4.

One general thing to note is that higher pressure does not necessarily mean higher particle impact velocities. This results from the fact that particle velocity is not only dependent on gas pressure but is affected by other factors, such as nozzle geometry, as described in Chapter 1. This leads to some interesting observations; for example, the particle (PA6) impact velocity with Gen III unit using a VRC Metal Systems regular 2 mm tungsten nozzle at 15 bar and 100 ^{o}C is 430 m/s, but at 25 bar and 100 ^{o}C, it is 409 m/s. In this case, the particle impact velocity is lower at a higher gas pressure. This is why the pressure rating of a cold spray system alone does not explain achievable impact

velocities, requiring more parameters to be accounted for. The exact reasons why the particle impact velocity decreased at higher pressure will be discussed in Chapter 3.

2.6 One-Dimensional Simulations

The theoretical particle impact velocities from Table 2 did not come from the datasheet of the cold spray units. Instead, these were simulated by a MATLAB script, which is a valuable tool for predicting the particle impact velocities that are practically difficult to measure without expensive, specialized diagnostic equipment. This MATLAB script uses the modeling methodology of Helfritch and Champagne [36], the convective heat transfer correlation described by Stoltenhoff et al. [37], and the bow shock effect described by Kosarev et al. [38]. To take into account the lower thermal conductivity of polymer particles compared to the metal powders, finite-rate conductive heat transfer was accounted for using the methods of Bacha et al. [39]. One-dimensional modeling has been used successfully for metal sprays, and it is comparable to CFD results [40].

MATLAB takes the main gas pressure and temperature as inputs, along with an initial particle temperature, permitting configurations with particle preheating, such as in the case of a benchtop unit. The script then requires gas and particle properties, along with the nozzle geometry. The script allows quick one-dimensional polymer cold spray simulations, which help predict and optimize the spray parameters. When the particle temperature is mentioned throughout Chapters 3 and 4, the average particle impact temperature is computed using this script.

When this thesis work was initiated, the limited study of polymer cold spray led to the initial development of a benchtop cold spray unit based on the design described by Bush et al. [6], a proven design that had worked with different polymers. This was the first working cold spray unit at Rowan University; it provided first-hand experience with many of the control parameters/variables and how they are interconnected. However, these process variables and interconnections are sensitive to system configuration, so it is essential to understand the cold spray control parameters and configuration types discussed in Chapter 1. This understanding is critical when setting up experiments focusing only on a particular aspect of cold spray. For this thesis, two specific areas studied were the velocity-temperature deposition window (Chapter 3) of PA6 powder and the effects of preheating the powder (Chapter 4).

Chapter 3

Experiments: Deposition Window Determination for PA6

3.1 Experimental Design

Initial cold spray experiments were conducted with the benchtop unit, which gave initial insights into how cold spray works and how it is controlled. Conditions for the initial proof of concept sprays, Figure 7, were determined by educated guesses, but as an understanding of the benchtop unit's performance increased, the experiments became more specific and focused on isolating single control parameters of the cold spray process. Initially, isolation was difficult to achieve because of the interconnectedness of the control parameters. However, more in-depth experiments were pursued once the benchtop unit could produce repeatable results. This chapter aimed to find the deposition window of a PA6 powder using the benchtop unit and the Gen III cold spray unit.

3.1.1 Powders

Throughout this chapter's deposition window experiments, the BASF Ultrasint PA6 X028 [33] powder was used because of its commercial availability in bulk and relatively low glass transition temperature (T_g) and melting temperature (T_m). The T_g and T_m values of this particular PA6 powder can be found in Table 3. Additionally, PA6 substrates were used throughout the experiments. These substrates were 3D printed by a Markforged Mark Two [41] printer, and the material used was Markforged F-MF-0003 [42]. Even though the base ingredient is PA6 for both the powder and the substrate,

additional compounding materials and the way of manufacturing were probable reasons for the difference in their T_g and T_m values.

Table 3

Properties of the PA6 Powder and PA6 substrate

	PA6 powder	PA6 substrate
Glass transition temperature T_g, °C	47.85 ± 2.98	25.77 ± 2.46
Melting temperature T_m, °C	215.98 ± 0.18	199.96 ± 0.43
Density, g/m^3	1.13	-
Specific heat, J/K*kg	1700	-
Thermal conductivity, W/m*K	0.26	-

Note. The T_g and T_m values are based on DSC measurements conducted at Rowan University. The density, specific heat, and thermal conductivity are from a manufacturer's datasheet [43] for PA6, which is expected to be similar to the BASF Ultrasint X028 powder used, but for which such information was unavailable.

3.1.2 Glass Transition Temperature

The glass transition temperature (T_g) is an interesting parameter for polymer cold spray. It is not an exact temperature but rather a temperature region where the reversible transition from a brittle glass-like state to a rubber-like state occurs [44]. This happens in amorphous polymers and amorphous regions of partially crystalline polymers [44]. Below T_g, the particles are relatively hard and brittle, leading to difficulties embedding

and mechanically interlocking on the substrate [45]. This is especially true with low-impact velocities since local thermal softening is challenging [45]. In the literature are some examples of the effects of T_g on the cold spray. Yang et al. [46] showed that critical velocity decreased significantly when the T_g of the polymer was decreased. Khalkhali et al. [8] also showed that materials with lower T_g deposits more easily and had higher deposition efficiencies. All of this suggests that the polymer's glass transition temperature should be considered when selecting polymer powders for cold spray, as it seems that lower T_g would facilitate deposition. Additionally, T_g might also be the temperature below, which meaningful deposition is not possible.

3.1.3 Deposition Window

The deposition window is defined as the space of cold spray processing conditions where a successful deposition on a substrate occurs. There are a lot of control parameters that contribute to the successful deposition in a cold spray process. In this thesis, particle impact temperature and particle impact velocity are the two control parameters focused on. The reason for using these two parameters is that the results could be generally compared to past research (e.g., Khalkhali et al. [8]) and are relatively easy to isolate and evaluate. To focus on these two parameters, the rest of the cold spray process control parameters had to be optimized (to an extent) and then fixed. Of those fixed parameters, two of the most important are the powder feed rate and the nozzle traverse speed. These have to be mentioned for a fair comparison of results because, in this thesis, a successful deposition – in simplest terms, a line of deposit formed by cold spraying – is defined as a deposition that occurs under a certain fixed powder feed rate

and traverse speed. This distinction is important because deposition could also be achieved by fixing the spray gun over the substrate so that a deposition only happens in one location. Though this could still be considered a deposition, the result is not practical in light of the applications where cold spray is used. As discussed in Chapter 1, cold spray has traditionally been used for coatings or repair, but recently, additive manufacturing has interested the manufacturing industry because of its intriguing potential [47]. All of these real-world applications use some feed rate and traverse speed combinations, and this is why it is important for this thesis to consider the successful cold spray deposition as dependent on feed rate and traverse speed, in addition to deposition window variables of particle impact temperature and particle impact velocity.

3.2 PA6 Deposition Window by the Benchtop Unit

As previously described, the first operational cold spray units at Rowan University were in-house-built benchtop units, versions one and two. The first version was primarily used for proof of concept, while the second, improved version was used for all the experiments described in this chapter. These experiments aimed to determine the deposition window of PA6 powder onto PA6 substrates, and the control parameters for the benchtop unit for these experiments were pressure and temperature of the main gas, traverse speed, powder feed rate, and nozzle stand-off distance. Out of those five control parameters, the traverse speed, the feed rate, and the stand-off distance were fixed to see how the main gas temperature and pressure affect the deposition window. The experimental main gas temperature and pressure can be converted into a calculated particle impact temperature and a calculated particle impact velocity by the one-

dimensional simulation described in Chapter 2; henceforth, the term "calculated" will not be stated unless needed for clarity. The traverse speed was fixed at 500 mm/min, the feed rate was set to the flow rate of powder corresponding to 60 PSI (the user's most directly controllable setting because of the pneumatic vibrator feed mechanism), and the nozzle stand-off from the substrate was 10 mm. Those values were preferred based on successful deposition events from previous experiments, though descriptions of these are beyond the scope of this work. Compressed air was used as the main gas, and a pressure regulator controlled it with a moisture trap to limit the moisture getting into the system.

The following steps were taken to find the deposition window of this PA6 powder. The powder was used as received; as described by Brennan et al. [10], there can be performance differences between as-received powder and prepared powder, but a more thorough discussion is beyond the scope of this thesis. The main gas pressure was kept between 1.4 and 4.8 bar, which are the lower and upper limits of the second benchtop unit. The main gas temperature was kept between 50 ^{o}C and 120 ^{o}C. The lower temperature limit was chosen based on the idea that deposition starts above the T_g of the powder, and the upper-temperature limit was selected because, above 120 ^{o}C, the powder began to clump in a powder feeder, affecting the feed rate. As described previously, this unit automatically preheats the powder, which means the main gas temperature equals the initial particle temperature. The substrate was not heated, but it was cleaned with isopropyl alcohol before the start of spray experiments.

The experiment was conducted as follows. The whole system was heated to a fixed main gas temperature, and when the correct powder temperature was reached,

measured by the thermocouple inside the hopper, a single line was sprayed at the 500 mm/min traverse speed onto a fresh patch of substrate. The main gas pressure was started at 1.4 bar, and after each line, it was increased by increments of 0.7 bar until 4.8 bar was reached. When the pressure sweep was done, the temperature was increased by 10 ^{o}C, and the process was repeated. This was done until the maximum system temperature of 120 ^{o}C was reached. The results of these experiments are shown in Figure 14.

To determine particle impact temperature and particle impact velocity as described in Chapter 2, the PA6 powder properties from Table 3 are used by the simulation; however, these parameters are not precisely for the BASF PA6 powder used. No data was available for this specific powder, so a different manufacturer's PA6 powder data was used [43]. This is not expected to significantly affect reported results, at best leading to a slight systematic bias in the results presented in Figure 14.

Figure 14

Deposition Window of the PA6 Powder by the Benchtop Unit

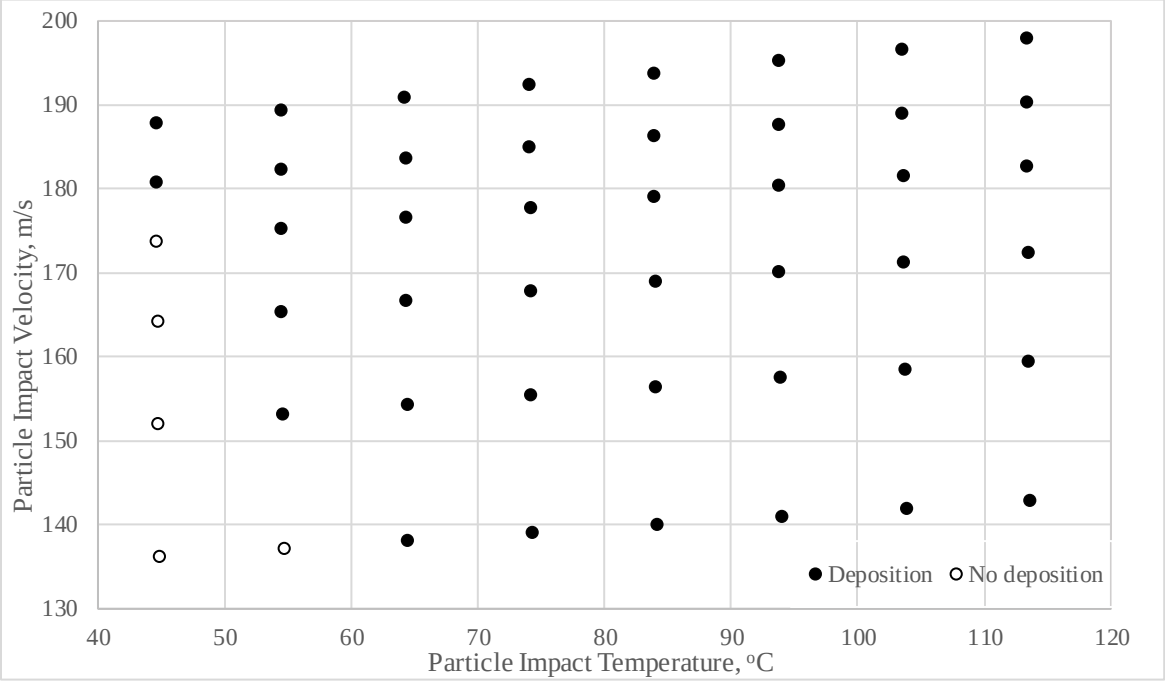

As shown in Figure 14, the experiments finding the deposition window of the PA6 powder appear to have been successful. However, "success" in determining a fixed deposition window will be further examined later in this thesis. The majority of the tested pressure and temperature combinations produced a successful deposition. The deposition started at a calculated particle impact temperature of 45°C, around the powder's glass transition temperature (47.85 ± 2.98 °C). This result aligns nicely with the hypothesis that the powder is relatively hard and brittle below the glass transition temperature and, therefore, difficult to deposit, especially under low particle impact velocities [45]. The usual metal cold spray particle velocities are between 300 and 1500 m/s, but the highest calculated velocity in this experiment was only ~198 m/s, which classifies this as a low-

velocity system. The critical velocity is the lowest particle impact velocity where successful deposition occurs. Critical velocity seems to be a curve affected by a particle impact temperature in this case. As the particle impact temperature increases, the critical velocity of the particles drops. Examples of successful sprays from these experiments are shown in Figure 15.

Figure 15

Examples of the Benchtop Unit Sprays

Note. a) main gas temperature 80 °C and air pressure 4 bar; b) main gas temperature 90 °C and air pressure 4 bar; c) main gas temperature 100 °C and air pressure 4 bar.

While this experiment was successful in probing the PA6 on the PA6 deposition window, exploration of the actual complete deposition window was limited because of the processing parameter limitations of the benchtop unit. For example, one way to increase particle impact velocities above ~200 m/s would be to use a supersonic nozzle; however, making such a nozzle in-house turned out to be complicated. To get around the significant engineering hurdles necessary to extend the benchtop unit's performance, a

different unit, The VRC Metal Systems Gen III Cold Spray System, with higher operating pressure and temperature ranges, was used with the same powder and substrate to widen the conditions space explored for the deposition window of PA6 powder.

3.3 PA6 Deposition Window by the Gen III

While the results from the benchtop unit appeared to establish a deposition window for PA6, they were also limited in terms of particle impact velocity. So, while a critical velocity curve might be inferred between the successful and unsuccessful deposition conditions (Figure 14), more testing at more diverse conditions was warranted. Research attention was given to the Gen III cold spray unit because it can reach higher particle impact velocities than the benchtop unit. As mentioned in Chapter 2, this unit was primarily designed for use with metal powders, but its wide parameter range (temperature and pressure) allows for polymer powder use.

Even though the Gen III could reach higher particle velocities, its particle impact temperatures were considerably lower because (1) its feeder was not preheated and (2) the geometry of the nozzles tested expanded and cooled gas from initial upstream conditions to achieve high-velocity downstream conditions. Once the first successful deposition of PA6 powder onto the PA6 substrate was achieved, this Gen III testing quickly evolved into a deposition window study. While the circumstances under which tests were performed may not be perfectly controlled scientific studies, they may instead be considered an exploration into what else is possible with this powder and substrate combination.

Determining the deposition of the PA6 powder was done just as it was with the benchtop unit. The control parameters were fixed except for the temperature and pressure of the main gas. The fixed parameters were determined based on the one-dimensional simulations, optimizations, and prior personnel experience with the Gen III cold spray unit. One of the most significant differences that had to be accounted for was the type of gas used. Gen III uses only nitrogen or helium, while the benchtop unit uses air. In this experiment, nitrogen was used as the main gas as it is quite similar to air from a gas dynamics standpoint. This substitution should not cause significant concern in comparing GEN III and benchtop unit data because the deposition window data from these two units is compared in terms of particle impact temperature and velocity, which are determined theoretically by the aforementioned one-dimensional particle simulation that already takes into account the type of gas used.

The wide particle impact velocity range for the Gen III results from the fact that it could be used at higher pressures and temperatures than the benchtop unit. In experiments presented here, the temperature of the main gas was limited by the melting point of the powder being sprayed. In the PA6 experimental results presented in Figure 16, the gas temperature had to remain below 200 ^{o}C because powder started to clog the applicator and the nozzle above this temperature. The pressure was limited in terms of the Gen III cold spray unit limitations and operational mode. For example, the nozzle had to have a throat above a specific diameter to use Gen III low-pressure mode (6.9 - 13.8 bar). For these tests, two nozzles were made based on the geometry of the nozzle used with the benchtop unit. One nozzle was made out of aluminum, and the other was 3D printed by

the same SLA printer used to print the powder feeder for the CSM-108, as discussed in Chapter 2. A tungsten carbide nozzle was used up to 44.82 bar in high-pressure mode to reach higher particle velocities.

One advantage of using air over nitrogen as cold spray propellant gas is that compressed air can be cheaply produced on location with a simple compressor. The fact that the Gen III unit used nitrogen became a limiting factor in how many sprays could be done during the experiment because only a limited amount of nitrogen cylinders could be attached to the Gen III unit during a single test campaign. This, coupled with limited access to the unit, resulted in only certain temperature and pressure combinations tested. Though more temperature and pressure combinations were not systematically explored, experiments presented here allowed for more extended testing of the deposition window for PA6 powder compared to the benchtop unit. The sprays were performed similarly to the benchtop unit's experiments, in which the main gas temperature was fixed until the chosen pressure sweep was conducted. The only difference in approach was that sprays were of multiple overlapping lines rather than a single line to determine the deposition. The combined results from these experiments and the benchtop unit experiments can be seen in Figure 16. An image of a sample spray from the Gen III experiments can be seen in Figure 17.

Figure 16

Deposition Window for PA6 Powder by the Benchtop Unit & the Gen III

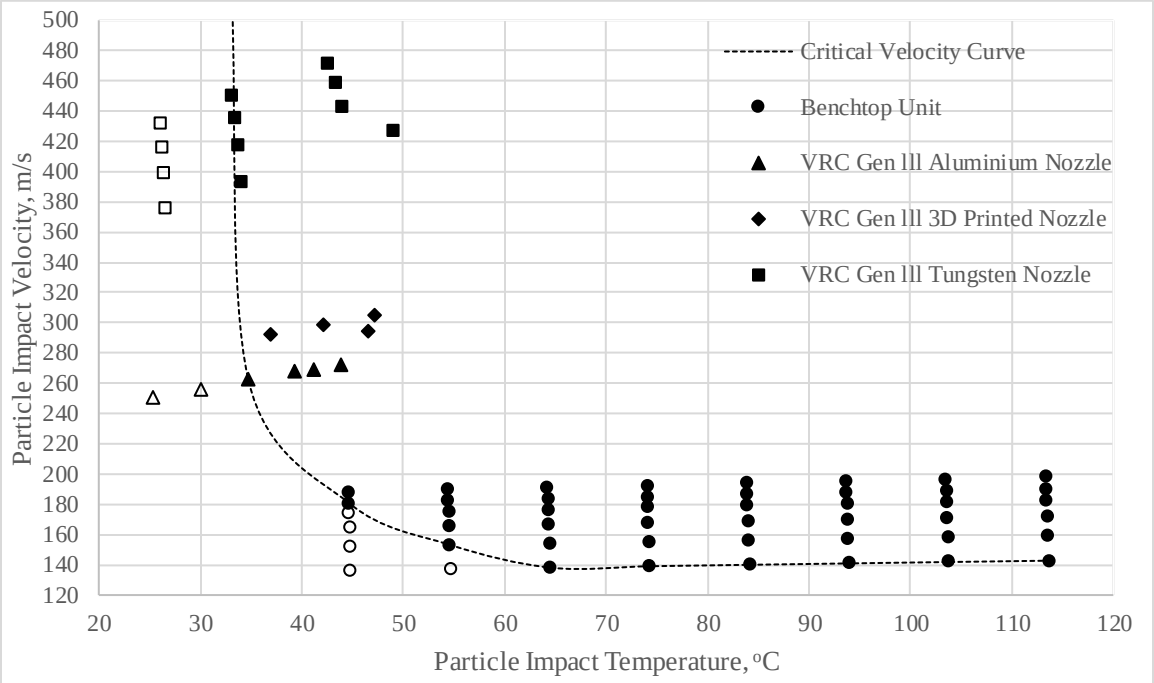

Note. Filled data points are successful deposition, and empty data points are unsuccessful deposition. The provided line is to guide readers' eyes – many other curve could also separate region of deposition (top and right) from region of no deposition (bottom and left).

Figure 17

Examples of the Benchtop Unit Sprays

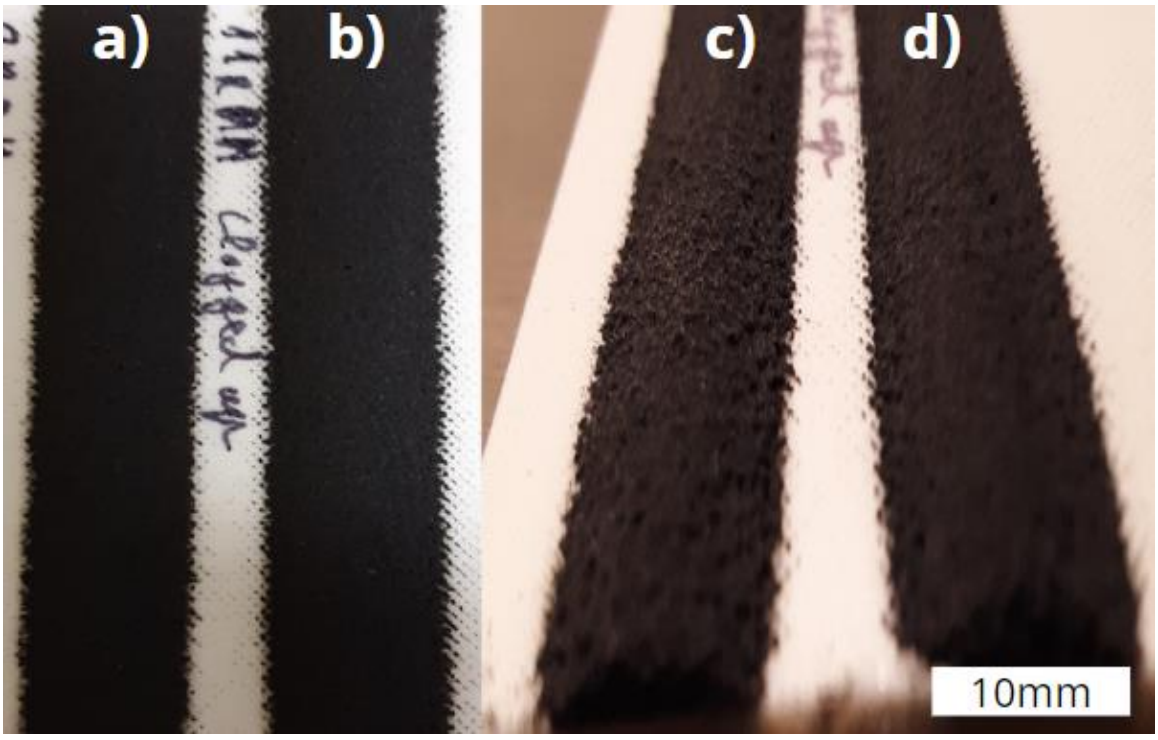

Note. a) main gas temperature 150 ^{0}C and air pressure 20.6 bar; b) main gas temperature 185 ^{0}C and air pressure 20.6 bar; c) main gas temperature 150 ^{0}C and air pressure 27.6 bar; d) main gas temperature 185 ^{0}C and air pressure 27.6 bar.

3.4 Analysis of the Results

Even though the Gen III experiment was quickly designed and executed, it produced exciting results. As shown in Figure 16, the apparent size of the deposition window of PA6 powder was increased in terms of particle impact velocity and temperature. The highest calculated particle impact velocity reached was ~471.5 m/s. As expected, the apparent trend in critical velocity continued, though more severely, as the

particle impact temperature decreased; a higher particle impact velocity was needed to have a successful deposition. The results also show that successful deposition was possible at calculated temperatures below the glass transition temperature of the powder. However, the lower limit for particle impact temperature seemed relatively constant at around 34 °C after the particle impact velocities of 270 m/s and greater. These observations create a clear, apparent critical velocity curve (Figure 16) that affects a particle's temperature. This needs further exploration with a single cold spray unit to keep as many parameters exactly the same as possible.

Another observation from the results presented in Figure 16 is that there are no data above/to the right of a particle impact velocity of 220 m/s and above a particle impact temperature of 50 °C. Even though the maximum main gas temperature of 200 °C was used, it only produced the highest particle impact temperature of 49 °C. Going above 200 °C was impossible because the nozzle and the applicator started to clog. In contrast, the benchtop unit could reach a particle impact temperature of 114 °C at 120 °C main gas temperature. The nozzle geometry plays an important role in particle impact temperature, as mentioned in Chapter 1, and the benchtop unit has a preheated powder feeder, while the Gen III does not. Accordingly, one way to further explore the effect of particle temperature by partially decoupling the effect of the nozzle is to adjust the particle impact temperature using a preheated/precooled powder feeder. This will be further discussed in Chapter 4.

When simulating the impact velocities of the Gen III experiments with the previously discussed MATLAB script, something interesting was noted - as the pressure

of the main gas reached a certain level, the particle impact velocity decreased while the particle impact temperature slightly increased. For example, the highest particle impact velocity of 471 m/s was reached at the main gas pressure of 21 bar, while at the highest main gas pressure of 45, the particle impact velocity was only 429 m/s. Such a difference was only observed when using the supersonic tungsten carbide nozzle. The reason for lower predicted velocities has something to do with an effect not yet mentioned in this thesis - a bow shock. As the high-velocity gas stream impinges on a substrate and gas becomes stagnant in front of the substrate, a shock wave forms in front of the substrate. The gas slows to velocities less than the particle velocity, causing a reversal in drag force direction on the particle, leading to a reduction in the particle velocity. At the same time, the gas behind the shock wave heats up, increasing the particle temperature [1]. This bow shock region is relatively small, and the velocity and temperature changes are minor except for very small and low-density particles [1]. Practically, the smaller particles can be limited by simply sieving the powder beforehand, but because of the low density of polymers, the bow shock might have a more significant effect in polymer cold spray than might be seen with metal cold spray. This effect needs to be kept in mind when designing a nozzle.

During the initial inspection, the Gen III experimental samples looked similar to benchtop unit deposits visually, but when it was time to analyze the deposition cross-section of both samples, something interesting was noted. The Gen III unit and benchtop samples are compared under a scanning electron microscope (SEM), and cross-sections of both samples are shown in Figure 18. The Gen III unit's sample was sprayed at a

particle impact velocity of ~427 m/s and a particle impact temperature of ~49 °C. The benchtop unit's sample was sprayed at a particle velocity of ~195 m/s and a particle impact temperature of ~94 °C. Simply looking at the samples, it could be said that the higher particle impact temperature produces less porosity. However, surprisingly, this was done at considerably lower particle velocities. This raises the question of the importance of preheated powders.

Figure 18

Cross-section View of the PA6 Deposits

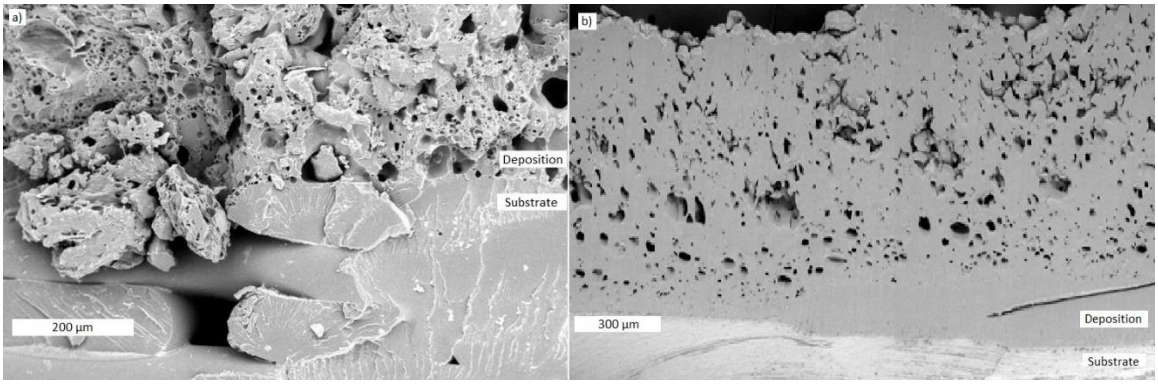

Note. A) is the Gen III sample, and B) is the benchtop unit sample.

The two experiments (Gen III and benchtop) showed that this particular PA6 powder can be successfully sprayed onto a PA6 substrate over a wide range of parameters. The two units are considerably different from each other, which presented some interesting results. The higher particle impact velocities of the Gen III unit showed that a successful deposition occurs well below the glass transition temperature of the powder. At the same time, higher particle impact temperatures produced by the benchtop

unit seemed to have a lower porosity of the sample deposits. The goal of both sets of experiments was to map out the PA6 powder's deposition window, but there is a large area above particle impact temperature of 50 ^{o}C and particle impact velocity of 200 m/s, which could not be accessed with these two units. A cold spray unit is required to achieve high enough particle impact velocities while maintaining the particle impact temperature. One way to do that is by preheating the powders to counteract the particles' cooling effect when they pass through the nozzle. Particle preheating could allow for expansion of the deposition window, along with its effects on the deposition quality and efficiency. This is the topic for Chapter 4.

Chapter 4

Experiments: Preheating

4.1 Introduction

Chapter 3 showed that PA6 can be successfully sprayed with an in-house built benchtop unit and a VRC Metal Systems Gen III Cold Spray unit originally designed for metal powders. Regardless of the success, there were a couple of shortcomings. First, the two units' limitations left a large region of particle impact velocities and particle impact temperatures excluded. Secondly, the differences in the units required the use of different control parameters like carrier gas, feed rate, and traverse speed. In order to deal with those shortcomings, a similar experiment with a different cold spray unit was designed. The cold spray unit used throughout the experiments described in this chapter was the CSM-108, which was described in Chapter 2.

4.2 Hardware

The CSM-108 is unique for a couple of reasons; first, even though it is a low-pressure system, it can reach relatively high particle impact velocities compared to the high-pressure Gen III unit. Secondly, the downstream injection feature of this unit removes the need for pressurized powder feeders, which makes it simple to use with different types of powder feeders. This is especially important for this experiment because the original powder feeder that came with CSM-108 could not produce a stable powder feed. It was replaced by a 3D-printed Gen III powder feeder replica as it showed

consistent feed rates through the previous experiments. A more detailed description of it appears in Chapter 2.

After the feed problem of the CSM-108 was solved, the next problem was how to reach the necessary particle impact temperatures and velocities to expand the deposition window of the PA6 powder, which was already determined in Chapter 3 for the benchtop unit. The answer to that was to preheat the powder before it was sprayed. There are two ways to do that: the entire powder feeder could be heated, or the powder on the way to the nozzle could be heated. The first option is similar to what happens in the benchtop unit. This design requires an insulated powder feeder with a heating element, which is relatively easy to design but could be time-consuming to reach the right powder temperature. The second option would only require heating the tubing through which the powder flows from the feeder to the nozzle. The second option was chosen because it was easier to accomplish. It was done using a 2-meter metal coil heated by the band heater and covered by special insulation. The setup can be seen in Figure 19. The necessary length of the tube was determined by CFD simulations based on the desired exit temperature of the particles. The heating of the coil before the experiment was relatively quick, especially compared to the time it took to start up the benchtop unit. In the end, it allowed quick and repeatable experiments with and without the preheating of the powders while keeping the control parameters the same.

Figure 19

Insulated Coil for Preheating the Powders

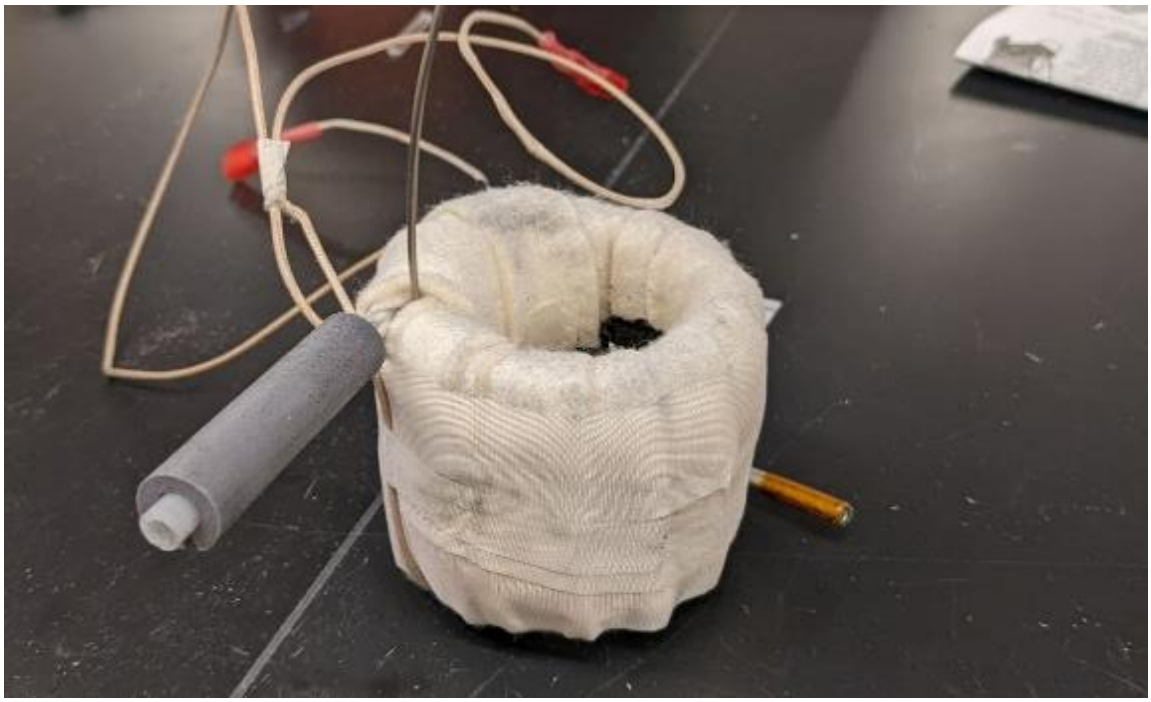

4.3 Experimental Setup

4.3.1 Deposition Window

When all the necessary modifications to CSM-108 were completed, the experiment finding the deposition window of the PA6 powder was continued. The powder was still the same PA6 described in Table 3, but a melt-cast PA6 substrate was used this time. The substrate change was due to the ease of acquiring the melt-cast substrate in large quantities and because the 3D-printed substrate had a relatively rough surface finish, which, in theory, could enhance the deposition. Figure 18 is an example of how it seems like a particle got stuck between the substrate layers without any visible

deformation. The effect of the substrate surface was discussed in Chapter 1.1.7. This is just another example of how many different parameters are involved in cold spraying and how difficult it is to control and test only a certain part of the spray system. The thermal properties of the new substrate were T_g = 40.25 ± 1.20 °C and T_m = 219.71 ± 0.18 °C. Those numbers are closer to the T_g and T_m of a PA6 powder Table 3.

The goal was to complete the deposition window experiment by reaching the missing particle impact temperature and velocities. That was achieved by using CSM-108 with a preheated powder feeder. The main gas used in this experiment was compressed air at 6, 8, and 10 bar pressures. Even though 12 bars is possible with this unit, the setup did not allow it to be used. The maximum temperature of the main gas was set at 150 °C because the nozzle started to clog above that temperature. Like the previous experiments, the rest of the spray parameters were fixed based on previous optimization experiments. That included the stand-off distance, feed rate of the powder feeder, and traverse speed. The substrate was cleaned with isopropyl alcohol and kept at room temperature, like in the previous experiments. The deposition was determined similarly to the benchtop unit experiment where the single line was attempted to be sprayed onto the substrate at constant traverse speed. The experiment was executed by fixing the main gas pressure and spraying a single line at each temperature from 150 °C downwards in 10 °C increments until there was no deposition. That was repeated until the temperature sweep was performed for each given pressure of 6, 8, and 10 bar.

The first experiment run was done without any preheating of the powder to get a baseline, but the same coil that was later used for preheating was attached the whole time

to keep the gas dynamics similar between the nozzle and the powder feeder throughout this experiment. After the no-preheating sprays were done, the coil was heated to the temperature of 100 ^{o}C, and the same pressure and temperature sweeps were done as before. The 100 ^{o}C coil temperature gave an initial particle temperature of 68 ^{o}C. Next, the coil temperature was raised to 150 ^{o}C at the coil, which gave 103 ^{o}C for the initial particle temperature. Again, the same pressure and temperature sweeps were performed, but it was difficult to execute this time. The powder tended to clog the nozzle or the powder entrance hole in the side of the nozzle. After each temperature sweep, the solution was to clean the coil and the nozzle. The initial particle temperature between those two sprays was quite large, leading to the third spray being done at the same temperature of 100 ^{o}C at the coil. However, this time, a different coil size gave an initial particle temperature of 84 ^{o}C. The same pressure and temperature sweep were conducted. That gave one data set at room temperature and three data sets at different initial particle temperatures.

By doing those experiments with the preheated powders, another question that was raised could be answered by using this data: What effect does the preheating of powders have on the deposition compared to non-preheated powders? This question comes from the fact that in Chapter 3, two different cold spray units were used, and one of the most significant differences between them was that the benchtop unit used preheated powders while Gen III did not. This is why the data collected in this experiment could be used to answer two questions. While collecting those 4 data sets, an exciting idea was brought up: what if the powder is cooled before reaching the nozzle?

This is not the most practical solution in manufacturing, but in the confines of this experiment, it might further help explain the effects of preheating the powders, and it might also be interesting to see how it affects the deposition window. The cooling of the particles could be done easily with the same setup, but this time, it could be done by covering the coil with dry ice. This was done by placing the coil into a beaker filled with dry ice and isopropyl alcohol. The resulting coil temperature was -78 ^{o}C, while the particle's initial temperature was determined to be -55 ^{o}C. The same pressure and temperature sweeps were performed with this cooling setup as were with the preheated powders. The results of all the experiments done in this chapter thus far can be seen in Figure 20, and the examples of different sprays can be seen in Table 4.

Figure 20

Results of the CSM-108 Sprays with Preheated Powder

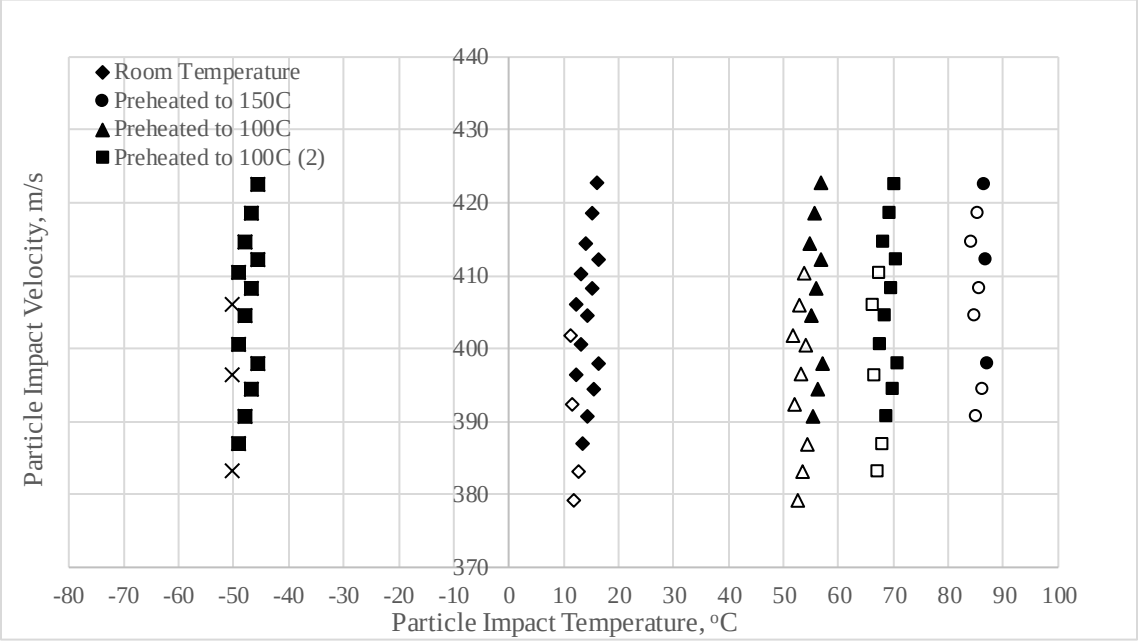

Note. Filled data points are successful deposition, and empty data points are unsuccessful deposition.

Table 4

Examples Spray Results from the CSM-108

System Temperature	Initial Particle Temperature -55 °C	Initial Particle Temperature 20.00 °C	Initial Particle Temperature 84 °C
110 °C 120 °C 130 °C 140 °C 150 °C	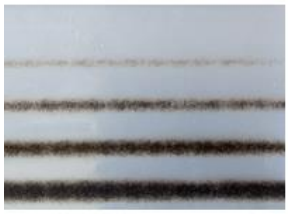	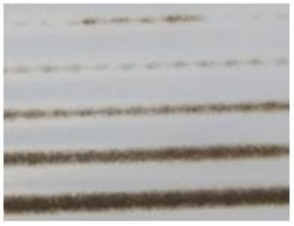	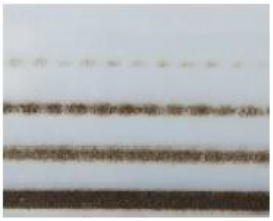

Note. The system pressure was 8 bar.

4.3.2 Deposition Efficiency

Parallel to the deposition window experiments, the deposition efficiency was measured to determine further the effect of the preheating and precooling of the powder. That was done only with the powders with the initial particle temperature of -54.95 °C, 20.00 °C, and 84.02 °C. Before describing the experiment, deposition efficiency had to be defined because there are multiple ways to measure it. Deposition efficiency could be measured between the substrate and the powder, or it could be measured between the already sprayed layer of powder and the powder that is sprayed. In this thesis, deposition efficiency was determined by considering both definitions. More precisely, a multiple-layer sample was sprayed, which combined the deposition efficiencies of both definitions. Deposition efficiency was calculated by Equation 2. That required weighting the substrate before and after the spraying to determine the weight increase of the sample. Also, the powder feeder was weighed before and after the spray to determine the total mass of material fired at the substrate. That is where the 3D printed feeder comes in handy because it can be kept on the scale throughout the spray, making the measuring super simple. The deposition efficiency was found between the same PA6 powder and the PA6 substrate used throughout this chapter. Again, all the control parameters are fixed except for the initial particle temperature that has already been mentioned. The near-optimized control parameters are as follows: main gas pressure of 6 bar, the main gas temperature of 150 °C, the stand-off distance of 20 mm, and the traverse speed of 2000 mm/min with a specific raster path. Each spray took about 3 minutes to complete, and for

each experiment setup, three samples were sprayed to get the most accurate results. An example of a deposition spray appears below in Figure 21.

Figure 21

Example of Deposition Efficiency Sprays

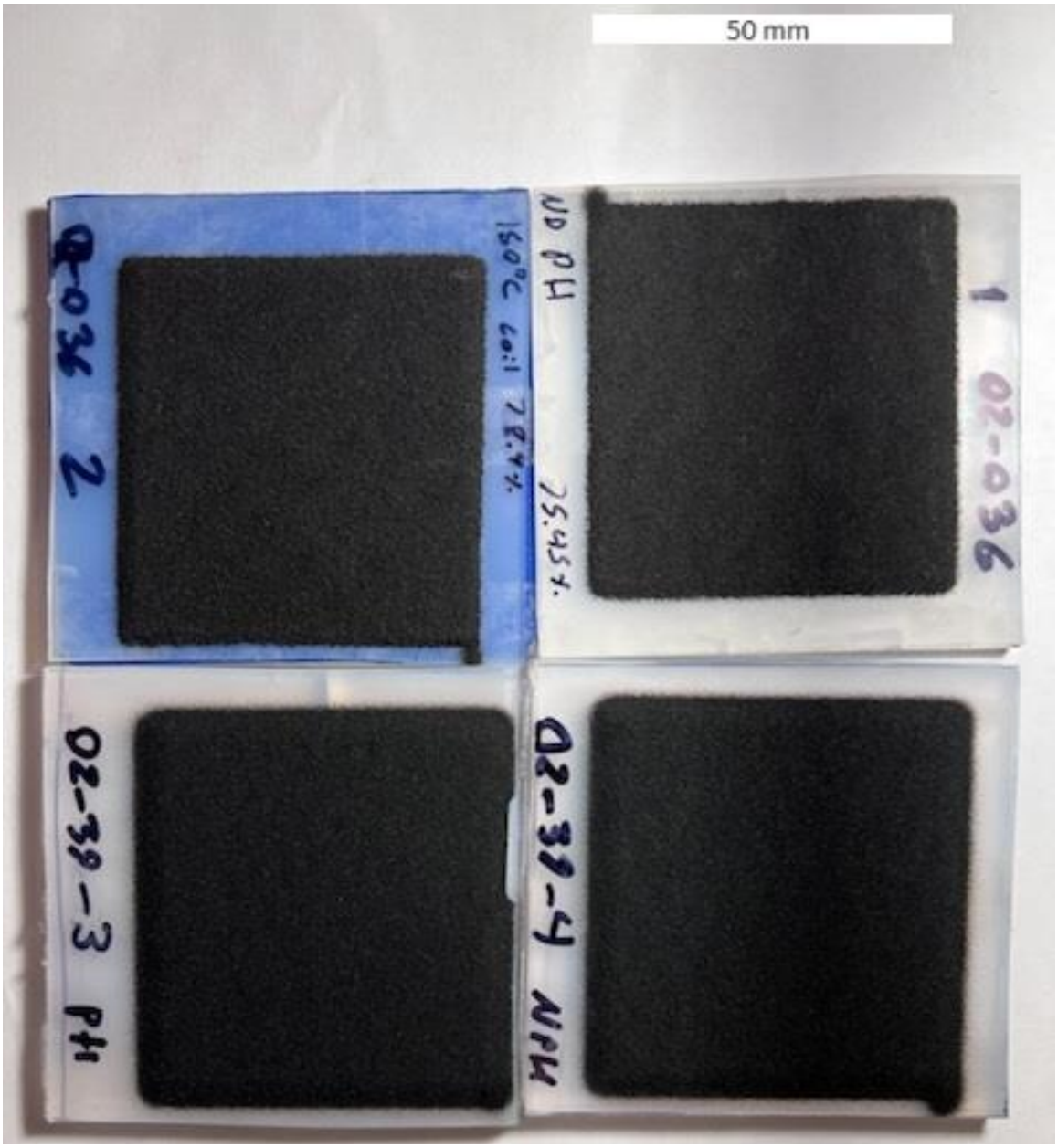

4.4 Analysis of the Results

4.4.1 Effects of the Preheated Powders

The CSM-108 experiments provided exciting results. The goal was to reach the particle impact temperatures and velocities that were impossible before and determine the effects of preheating the powders. First, the effects of the preheating are analyzed. Figure 20 shows a relatively clear critical velocity line between 386.97 m/s and 397.95 m/s could be drawn. That means that the preheating of powders, in this case, seems to have a negative effect on the deposition window, meaning that higher critical velocity is needed to achieve a successful deposition as the particle impact temperature rises. When the data from the 150 ^{o}C preheating is excluded, the critical velocity difference between the room temperature and preheated experiments only became 3.7 m/s. Based on that, it could be stated that the critical velocity difference is too small to definitively say that preheating of powders makes a significant difference when determining the deposition window. The reason for excluding the 150 ^{o}C data was that the clogging of the nozzle and the preheated coil was a constant problem that might have impacted the results during the experiment. When considering the data from the cooling experiment, the critical velocity is very similar to the no-preheating experiment; the actual spray comparison can be seen in Table 4, where the no-preheat experiment was able to deposit under a slightly lower system temperature. Regardless, the differences are quite small, and it can be concluded that with this setup, the preheating of powder particles has minimal effect on the deposition window.

The deposition efficiency results can be seen in Table 5. From the results, the difference between the deposition efficiencies is around 3% with a few percent deviation, which means there is no substantial statistical difference between them. Based on that, it can be concluded that the pre-heating or precooling has no significant effect on deposition efficiency.

Table 5

Deposition Efficiency Results

	Initial Particle Temperature -54.95 °C	Initial Particle Temperature 20.00 °C	Initial Particle Temperature 84.02 °C
Deposition Efficiency	67.38 ± 2.58%	64.78 ± 1.42%	67.78 ± 3.07%

The preheating or the precooling of the particles does not seem to affect the deposition window or efficiency. Even though the preheating of powders does not look like it has any effect on the deposition window and deposition efficiency, it still allows for reaching particle impact temperatures and velocities that were not possible before. As a result, the data collected in Chapter 3 could be improved by including the preheating data in Figure 20.

4.4.2 Final Deposition Window Results

At the end of Chapter 3, a relatively clear critical velocity curve could be drawn based on the data collected by the benchtop and the Gen III cold spray units, as seen in

Figure 16. One of the motivating factors for using the CSM-108 cold spray unit with preheated powders was to expand that deposition window (Figure 16). The data collected in Chapters 3 and 4 are combined in Figure 22.

Figure 22

Final Deposition Window Results

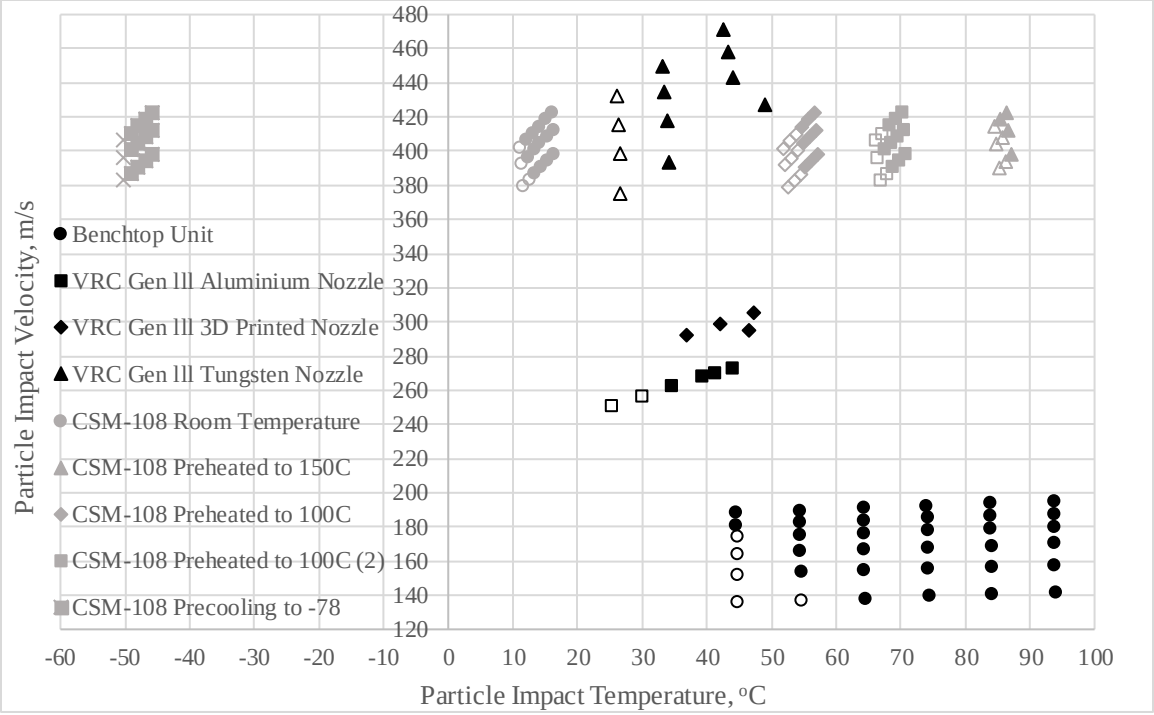

Note. Filled data points are successful deposition, and empty data points are unsuccessful deposition.

The additional data from the CSM-108 greatly complicates the results, and this once apparent critical velocity curve observed in Figure 16 is gone. The data from CSM-108 is all over the place for multiple reasons. One of the best comparisons is the Gen III

tungsten carbide nozzle experiment and the CSM-108 no preheat experiment data. Both experiments used powders at room temperature, and the CSM-108 had a successful deposition at the particle impact temperature of 15 °C and the particle impact velocity of 394 m/s, while the Gen III unit had a first successful deposition at the particle impact temperature of 34 °C at a particle impact velocity of 393 m/s. That means the CSM-108 had a successful deposition around the same particle impact velocity but at around 19 °C lower particle impact temperature. That is a considerable difference. It did not stop there; the CSM-108 was able to successfully deposit PA6 powder outside of the previously determined critical velocity curve, even with negative (in °C) initial particle temperatures.

Even if the data outside of the previously determined critical velocity curve is excluded, the rest of the data does not align with the data collected in Chapter 3. The data from the strictly preheated experiments did not produce any successful deposition below the particle impact velocity of 390 m/s. That was unexpected because, based on previous data, it seemed perfectly reasonable to have successful deposition around that area. For example, looking at the CSM-108 preheat 100 °C data from Figure 22, the CSM-108 system could not deposit anything below 53 °C of particle impact temperature regardless of the particle impact velocity. At the same time, roughly at the same particle velocity of 393 m/s, the Gen III tungsten carbide nozzle experiment successfully deposited at 34 °C of particle impact temperature. Again, that difference is around 19 °C, but this time, the other way in terms of which unit could deposit and which could not.

Another peculiarity about the CSM-108 data was that those results are so bunched together, and the differences between the successful and unsuccessful deposits are

minimal. It almost forms an independent data cluster at each parameter combination, as seen in Figure 22. To point out how minor the differences between the successful and unsuccessful deposition within a single cluster are, the CSM-108 room temperature data is examined. The two highlighted sprays in Figure 23, where one is unsuccessful and the other is successful, have similar particle impact velocities of 402 m/s and 401 m/s, respectively, with their particle impact temperatures were 11 ^{o}C and 13 ^{o}C, respectively. That leaves only a 1 m/s difference between the velocities and a 2 ^{o}C difference between the temperatures to determine the deposition window. This is just one example; similar observations can be made through the CSM-108 data clusters. These results show that the simple particle velocity-temperature charts might not be enough to determine the deposition or no deposition.

Figure 23

Room Temperature Spray Results from CSM-108 Experiment

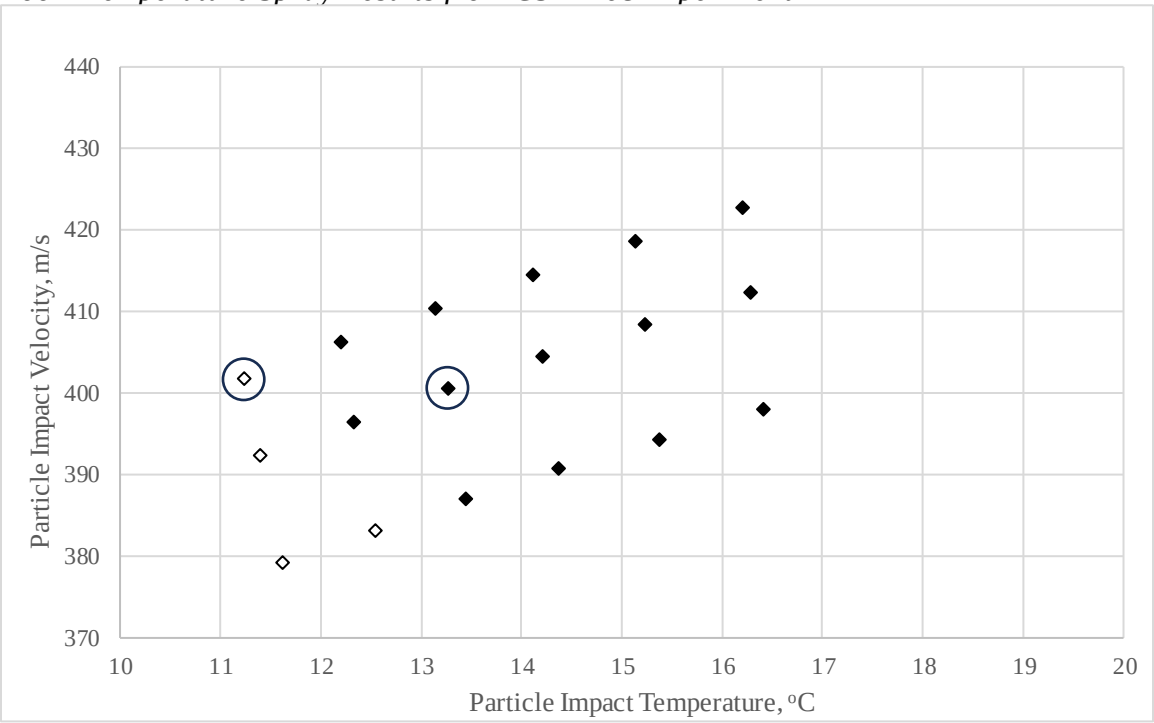

Note. Filled data points are successful deposition, and empty data points are unsuccessful deposition.

4.5 Validity of the Experiments

4.5.1 Effects of the Preheated Powders

Based on the results seen in Chapter 3, there might be a difference between preheating and not preheating the powders before the spray. SEM results pointed towards the lower porosity of the preheated spray samples, plus preheating allowed lower critical velocities for a successful deposition. That was put to the test by a CSM-108 unit that allowed for preheated and not preheated powders to be sprayed at the same spray

conditions. As previously demonstrated, the effect of the preheating or cooling of the particles is limited and statistically nonexistent for deposition window and deposition efficiency. The fact that there was such a big difference in the results between the CSM-108 experiments and the benchtop and the Gen III experiments led to further analysis of the experiment setup and the cold spray units.

The only way to directly compare the results of the three cold spray units was to convert the data into the same two variables with the help of the previously mentioned one-dimensional MATLAB script. Some accuracy questions about this approach will be discussed later in this chapter. The experiments were set up as similarly as possible, but one of the more significant differences was the different substrates used in the CSM-108 experiments. In terms of the effects of the preheating of powders, this should not play such a crucial role simply because the difference in the substrates should only affect the conditions under which the deposition happens, but the effect on the preheat should still be noticeable even if the conditions for successful deposition might be slightly different than with benchtop and Gen III experiments. Those substrates were still PA6-based, and T_g and T_m were similar to the previous substrates. The different substrates could slightly affect comparing the CSM-108 to benchtop and Gen III results, but CSM-108 results alone are valid.

The most significant difference between the experiments is the cold spray units themselves. The fact that the Gen III and benchtop units are upstream injection systems and the CSM-108 unit is a downstream injection system might play a role here. The difference between the upstream and downstream injection systems was described in

Chapter 1. The CSM-108 nozzle is designed so that the powder is "sucked" into the nozzle from the side, and that seems to cause the powder to hit the opposite wall of the nozzle. That could lead to particle deformation, which, in turn, can lead to changes in the morphology and size distribution of the particles. As explained in Chapter 1, the morphology and size distribution of the powder does affect the particle temperatures and velocities. This wall effect is nonexistent in the upstream injection systems. This simple design feature of the CSM-108 nozzle could change the conditions under which the deposition occurs, but the overall effect on the preheating should still be seen. As a side note, this nozzle design might explain why there was a slight increase in critical velocity as the initial particle temperature was increased. It can come down to the simple fact that higher initial particle temperature causes increased deformation when they hit the other side of the nozzle wall. That also would explain why, during the 150 ^{o}C preheat sprays, the constant clogging of the nozzle happened.

Another observation made during the deposition efficiency sprays with the CSM-108 was that some substrate preheating occurred during the spray cycle. For the DE spray experiments, the raster path had a stepover between the lines of 1 mm, which means that individual spray lines overlap each other after each pass. During the sprays, what seemed to be happening was that the first line of the spray was spotty, but as more lines were laid down, they started to look better. What might have happened there was that the main gas was constantly heating the substrate, and because of the large number of lines sprayed in a single experiment, the local heating of the substrate might have been considerable.

In the end, it seems like the CSM-108 data about the preheating should be correct, and it looks like the preheating or cooling of particles has statistically no effect on the deposition window or deposition efficiency with this specific unit and powder/substrate system. This does not mean the preheating of powders does not affect other parts of the deposition. For example, the higher porosity results of the preheated powders were mentioned in Chapter 3; the CSM-108 did not specifically test this. Another way to judge the deposition would be mechanical testing. In the literature, it has been done before and with a preheated powder, which led to mechanical properties similar to those of the cold spray samples compared to the melt cast samples. Maybe the preheating of powders was one of the important factors for the success. It was further explained in section 1.2. Unfortunately, the porosity and the mechanical testing of the samples were beyond the scope of this thesis.

4.5.2 Final Deposition Window Results

The results were surprising compared to previous experiments, but the data is valid in terms of this specific experiment with the CSM-108. The results are all over the place when examining the deposition window data from Figure 22. This raises the question of whether comparing the data between three different units is fair.

The comparison was possible based on a temperature-velocity deposition window because all the deposition data were converted into the same parameters - particle impact temperature and velocity. Impact parameter estimation was done using the MATLAB script discussed in Chapter 2. As already mentioned, the one-dimensional simulation has shown excellent results when predicting the parameters of the metal powders [40], but the

accuracy of predicting the parameters of the polymer powders can be questioned for various reasons [6, 39]. Initial cold spray control parameters like system pressure and temperature can not be used for the comparison because many other parameters affect the final result. All those different parameters were mentioned in Chapter 1. The MATLAB script does its best to take all of them into account, but because there are so many variables that, in some cases, are interconnected, there needs to be some simplification and assumptions in the simulation.

A great example of one variable present in experiments but simplified in model interpretation is the powder size distribution, which, in the case of the MATLAB script, is nonexistent because an average particle size is used. However, this factor is important because the effect of the particle size can be huge. For example, in the CSM-108 spray at a system pressure of 8 bar and temperature of 120 ^{o}C, a 75 μm particle is estimated to reach a velocity of 400 m/s upon impact. In contrast, a 55 μm particle reaches a velocity of 418 m/s upon impact. In this example, the particle impact temperature at 75 μm particle size is 13 ^{o}C and at 55 μm 11 ^{o}C. The velocity and temperature difference between the particle sizes can lead to instances where only a certain size of particles deposits because they only have sufficient critical velocity. The particle impact temperature estimated in the MATLAB script is also an average temperature, which means that different layers inside the particle can have different temperatures. Combining this with the critical velocities for each spray condition, we might only have a specific particle size depositing depending on the critical velocity and particle impact temperature. What makes it harder to judge is that the deposition looks the same visually

and can still be called a successful deposition. That can mislead the results, especially when the difference between a successful and unsuccessful deposition is a couple of degrees or meters per second, just as in Figure 23.

Additionally, the particle size distribution for this PA6 powder used throughout the experiments in this thesis has a mean particle size D50 of 75 μm. D50 means that by volume, 50% of the particle diameters are equal to or smaller than 75 μm [1]. This is the size distribution of the entire bag of powder, but the small samples of it that are used in a powder feeder can have different size distributions each time they are filled. That can easily lead to a different result with the same fixed parameters. Unfortunately, commercial powders, most of the time, come in large distribution sizes.

Because of gas heating/cooling and expansion details, simulation is the best way to compare data from multiple cold spray units. If we take a step back, there are considerable setup differences between the experiments with each cold spray unit. Those differences were dictated by the differences and the limitations of the units. They all had slightly different feed rates and traverse speed combinations; the CSM-108 used different substrates, and Gen III used N_2 as the main gas. Those decisions were necessary to spray polymer with those cold spray units successfully. Figure 22 shows that data from the benchtop and Gen III units line up reasonably well, and the effect of particle velocity and temperature can be seen. It is the CSM-108 data that mixes everything up in terms of determining the deposition window for this PA6 powder. When comparing those units, the CSM-108 has a downstream injection system, while the others have an upstream injection system. Those effects were discussed earlier, but could the specific nozzle

design of the CSM-108 be the determining factor? This nozzle seems designed to be as simple as possible and work under limited conditions (in terms of particle impact temperature and velocity), as seen in Figure 22, where all the data is bunched together compared to the other cold spray units' data. That is achieved even though the main gas's pressure and temperature can be manipulated considerably. Those tight data sets remained consistent even when different initial particle temperatures were tested. The reason for such a tight range of the particle impact temperature and velocity could be because, initially, this unit had inaccurate control over the control parameters, and possibly, to limit user errors, this CSM-108 cold spray unit was designed and optimized only for specific applications.

Chapter 5

Conclusion

This thesis aimed to explore and expand the capabilities of polymer-on-polymer cold spray using polyamide 6 (PA6) powder and substrates and three different cold spray systems (benchtop unit, Gen III, and CSM–108). These units were described in Chapter 2. An initial goal of this work was to determine the deposition window and deposition efficiency of the PA6 powder, and the advantage of having multiple cold spray systems allowed testing of a larger range of process control parameters (such as inferred particle impact temperature and impact velocity) along with the different styles for powder injection. However, results presented in Chapters 2-4 of this thesis indicated that a simple definition of a deposition window for the PA6 system may not apply among different cold spray facilities.

The combination of experiments performed with these three different cold spray units produced a large deposition window for PA6 powder (summarized in Figure 22). The differences between the units did not allow direct comparison among the results indicated by system operating parameters such as system temperature and pressure. Instead, results had to be interpreted using a simple one-dimensional MATLAB simulation script (described in Section 2.6) to harmonize all of the data in terms of particle impact temperature and particle impact velocity. Even after data was scaled to these common variables, the deposition window results from the different cold spray units appeared contradictory, especially the CSM–108 deposition window results.

Restricting attention to the Figure 16 partial deposition window results for only the benchtop and Gen III experiments, a clear boundary is evident in terms of inferred particle impact velocity and particle impact temperature above which PA6 deposition was possible. These results suggest that the critical velocity (minimum particle velocity above which the deposition is successful) has a significant dependence on the particle impact temperature. The benchtop unit uses preheated powder by design, allowing it to reach high particle impact temperatures while keeping the impact velocities low. Successful deposition for the benchtop unit happened around 140 m/s, which is about 120 m/s lower than the lowest particle impact velocity that produced a successful deposition for the Gen III cold spray unit. The apparent trade-off between these two systems is thermal energy versus kinetic energy; however, much of the higher temperature and higher velocity space could not be explored due to system operating limits.

The downstream configuration of the CSM-108 provides a different thermal history for the powder than for the other two systems, and modifications to the base CSM-108 unit also permitted the study of preheated/precooled and room-temperature powders. These capabilities provided access to the temperatures and velocities of deposition window space that were not previously accessible to the benchtop and Gen III units. However, for many reasons discussed in Section 4.5, the results from the CSM–108 did not fit neatly inside the deposition window results for the benchtop unit plus the Gen III unit. In addition, CSM-108 results with preheated powder indicated no statistically significant difference in deposition efficiency between preheated and non-preheated powder sprays. If anything, preheating made the spraying more difficult with this cold

spray system, as discussed in Section 4.4. The combined deposition window results from all three systems show that particle impact velocity and particle impact temperature alone may be too simple to describe simple regions of deposition/no deposition. Additional factors for deposition that may be considered in the future include the thermal history of the particle, particle morphology and size, and particle injection methods, among others; however, this is beyond the scope of the present thesis.

As previously mentioned, determining deposition efficiencies for the PA6 powders was a second objective for this thesis. During the aforementioned CSM–108 preheating experiments, the deposition efficiency for PA6 during preheated, precooled, and room-temperature powder sprays was a roughly constant value of 67%. This is over six times higher than the highest previously published polymer-on-polymer cold spray deposition efficiencies described in the literature (LDPE powder on HDPE substrate) [6, 8] when these PA6 experiments were conducted. That is quite a significant jump, especially considering the benchtop unit's deposition efficiency with the same PA6 powder was around 1%. Discovering the exact reasons for the high deposition efficiencies seen with the CSM-108 sprays merits attention beyond the scope of this thesis, but some consideration should be given to the fact that this specific PA6 powder has been compounded with additives and otherwise optimized as a laser sintering powder. Similarly, the manner of powder injection might play a role in the favorable deposition efficiency results. Regardless, the CSM-108 results represent a huge improvement in terms of deposition efficiency in polymer-on-polymer cold spray.

Ultimately, the goals set at the beginning of this thesis were achieved. The polymer was successfully sprayed onto polymer substrates, and the deposition efficiency increased roughly 6.7 times [6, 8]. The most significant factor in determining conditions for successful deposition was the access to different cold spray systems. These permitted insight into different ways to achieve cold spray and how interconnected the process control parameters were. Present results clearly show that understanding the control parameters is a must when setting up, interpreting, and comparing cold spray experiments.

5.1 Future Work

Overall, the overarching questions posed by this thesis regarding deposition window and deposition efficiency were addressed above. Still, throughout this thesis, a number of additional questions were raised as topics for future work.

Broadly speaking, systematic optimization of the cold spray process for a particular powder and substrate was beyond the scope of this thesis. The main control parameters and response metrics were the inferred impact velocity, impact temperature, and the presence/absence of deposition. However, the present results serve to indicate that the target of optimization itself requires a clear definition. For example, favorable deposition efficiency (even beyond the binary limits of a deposition window) does not guarantee favorable porosity or mechanical strength in the cold spray deposit.

Specifically indicated in this work, further research into the effects of powder and substrate preheating and their effects in terms of porosity and adhesion strength is

warranted. Higher-density deposits could lead to higher deposit strength, which various mechanical tests could easily determine.

Also, systematic preheating experiments should be done to compare upstream injection cold spray with a downstream injection cold spray where the injection tube runs through the nozzle's throat to avoid any possible particle deformations before hitting the substrate. Such experiments could confirm the cold spray experiments previously described in this thesis and paint a clearer picture of the effects/non-effects of different cold spray systems. A real case could be made that one type of cold spray configuration is more suitable for polymer-on-polymer cold spray.

Though investigations in this thesis were limited in scope, previously discussed results indicate that a couple of other important control parameters affecting results are the size distribution and morphology of the powder. As one control parameter, the powder should be prepared beforehand in terms of the size distribution (i.e., through sieving). In terms of the deposition window, there could be a case where only particles of certain sizes are deposited under certain system settings. Unconditioned powder can lead to misleading results, in some cases indicating successful deposition, while in others, using a different sample of the same powder under the same spray conditions, deposition may not be successful because of powder size distribution partitioning during storage and handling.

Other factors around the storage, handling, and conditioning of powder (e.g., moisture control) were considered in the present work and have been more thoroughly discussed in the work of Brennan et al. [10]. Nevertheless, the present conclusion that

particle impact velocity and particle impact temperature are insufficient to describe deposition/no deposition conditions suggests that further investigation into powder conditioning may be helpful for consistent polymer cold spray results.

The powder's presence/absence of chemical additives is somewhat related to this idea. In the present work, the PA6 powder used was BASF Ultrasint X028, which is composed of a PA6 base plus unknown additives presumably tailored to improve the laser sintering process for which this powder was developed. While experiments conducted in this thesis compared BASF Ultrasint X028 results to other BASF Ultrasint X028 results, this did not permit an understanding of the effect of these additives compared to a chemically "pure" PA6. Comparing deposition windows of pure and modified polymer powders could inform particle formulation strategies for more optimal cold spraying results.

References

[1] V. K. Champagne, O. C. Ozdemir, and A. Nardi, *Practical Cold Spray*. Springer International Publishing, 2021.

[2] J. Villafuerte, *Modern Cold Spray Materials, Process, and Applications*, 1st 2015. ed. Cham: Springer International Publishing, 2015.

[3] A. Papyrin, *Cold spray technology*. Amsterdam: Elsevier, 2007.

[4] J. Karthikeyan, "4 - The advantages and disadvantages of the cold spray coating process," in *The Cold Spray Materials Deposition Process*, V. K. Champagne Ed.: Woodhead Publishing, 2007, pp. 62-71.

[5] A. Moridi, S. M. Hassani-Gangaraj, M. Guagliano, and M. Dao, "Cold spray coating: review of material systems and future perspectives," *Surface Engineering*, vol. 30, no. 6, pp. 369-395, 2014/06/01 2014, doi: 10.1179/1743294414Y.0000000270.

[6] T. B. Bush, Z. Khalkhali, V. Champagne, D. P. Schmidt, and J. P. Rothstein, "Optimization of Cold Spray Deposition of High-Density Polyethylene Powders," *Journal of Thermal Spray Technology*, vol. 26, no. 7, pp. 1548-1564, 2017/10/01 2017, doi: 10.1007/s11666-017-0627-5.

[7] Y. Xu and I. M. Hutchings, "Cold spray deposition of thermoplastic powder," *Surface and Coatings Technology*, vol. 201, no. 6, pp. 3044-3050, 2006/12/04/ 2006, doi: https://doi.org/10.1016/j.surfcoat.2006.06.016.

[8] Z. Khalkhali and J. P. Rothstein, "Characterization of the cold spray deposition of a wide variety of polymeric powders," *Surface and Coatings Technology*, vol. 383, p. 125251, 2020/02/15/ 2020, doi: https://doi.org/10.1016/j.surfcoat.2019.125251.

[9] T. Bacha, D. Brennan, Ü. Tiitma, F. Haas, and J. Stanzione, "Effects of Powder Feedstock Pre-Heating on Polymer Cold Spray Deposition," in *ITSC2022*, 2022: ASM International, pp. 44-55.

[10] D. Brennan, T. Bacha, Ü. Tiitma, F. Haas, and J. Stanzione, "Systematic Study of the Effects of Powder Preconditioning on Flowability and Deposition in Polymer Cold Spray," in *ITSC2022*, 2022: ASM International, pp. 683-694.

[11] J. Davis, "Cold spray process," *Handbook of Thermal Spray Technology, ASM International*, pp. 77-84, 2004.

[12] K. Balani, A. Agarwal, S. Seal, and J. Karthikeyan, "Transmission electron microscopy of cold sprayed 1100 aluminum coating," *Scripta Materialia*, vol. 53, no. 7, pp. 845-850, 2005/10/01/ 2005, doi: https://doi.org/10.1016/j.scriptamat.2005.06.008.

[13] D. MacDonald, S. Rahmati, B. Jodoin, and W. Birtch, "An Economical Approach to Cold Spray Using In-line Nitrogen–Helium Blending," *Journal of Thermal Spray Technology*, vol. 28, no. 1, pp. 161-173, 2019/01/01 2019, doi: 10.1007/s11666-018-0813-0.

[14] L. Binek and A. T. Nardi, "Hydrogen Based Cold Spray Nozzle and Method," 2017. [Online]. Available: https://www.freepatentsonline.com/20190024242.pdf

[15] H. Koivuluoto, A. Coleman, K. Murray, M. Kearns, and P. Vuoristo, "High Pressure Cold Sprayed (HPCS) and Low Pressure Cold Sprayed (LPCS) Coatings Prepared from OFHC Cu Feedstock: Overview from Powder Characteristics to Coating Properties," *Journal of Thermal Spray Technology*, vol. 21, no. 5, pp. 1065-1075, 2012/09/01 2012, doi: 10.1007/s11666-012-9790-x.

[16] H. Assadi, F. Gärtner, T. Stoltenhoff, and H. Kreye, "Bonding mechanism in cold gas spraying," *Acta Materialia*, vol. 51, no. 15, pp. 4379-4394, 2003/09/03/ 2003, doi: https://doi.org/10.1016/S1359-6454(03)00274-X.

[17] H. Assadi, H. Kreye, F. Gärtner, and T. Klassen, "Cold spraying – A materials perspective," *Acta Materialia*, vol. 116, pp. 382-407, 2016/09/01/ 2016, doi: https://doi.org/10.1016/j.actamat.2016.06.034.

[18] D. Helfritch and V. Champagne, "A model study of powder particle size effects in cold spray deposition," Army Research Lab Aberdeen Proving Ground MD, 2008.

[19] W. Wong, P. Vo, E. Irissou, A. N. Ryabinin, J. G. Legoux, and S. Yue, "Effect of Particle Morphology and Size Distribution on Cold-Sprayed Pure Titanium Coatings," *Journal of Thermal Spray Technology*, vol. 22, no. 7, pp. 1140-1153, 2013/10/01 2013, doi: 10.1007/s11666-013-9951-6.

[20] V. K. Champagne, "1 - Introduction," in *The Cold Spray Materials Deposition Process*, V. K. Champagne Ed.: Woodhead Publishing, 2007, pp. 1-7.

[21] S. Yin, X.-f. Wang, W. Y. Li, and H.-e. Jie, "Effect of substrate hardness on the deformation behavior of subsequently incident particles in cold spraying," *Applied Surface Science*, vol. 257, no. 17, pp. 7560-7565, 2011/06/15/ 2011, doi: https://doi.org/10.1016/j.apsusc.2011.03.126.

[22] J. G. Legoux, E. Irissou, and C. Moreau, "Effect of Substrate Temperature on the Formation Mechanism of Cold-Sprayed Aluminum, Zinc and Tin Coatings," *Journal of Thermal Spray Technology*, vol. 16, no. 5, pp. 619-626, 2007/12/01 2007, doi: 10.1007/s11666-007-9091-y.

[23] P. Richer, B. Jodoin, and L. Ajdelsztajn, "Substrate roughness and thickness effects on cold spray nanocrystalline Al–Mg coatings," *Journal of Thermal Spray Technology*, vol. 15, no. 2, pp. 246-254, 2006/06/01 2006, doi: 10.1361/105996306X108174.

[24] T. Marrocco, D. G. McCartney, P. H. Shipway, and A. J. Sturgeon, "Production of titanium deposits by cold-gas dynamic spray: Numerical modeling and experimental characterization," *Journal of Thermal Spray Technology*, vol. 15, no. 2, pp. 263-272, 2006/06/01 2006, doi: 10.1361/105996306X108219.

[25] X. Wang *et al.*, "Characterization and modeling of the bonding process in cold spray additive manufacturing," *Additive Manufacturing*, vol. 8, pp. 149-162, 2015/10/01/ 2015, doi: https://doi.org/10.1016/j.addma.2015.03.006.

[26] A. Ganesan, J. Affi, M. Yamada, and M. Fukumoto, "Bonding behavior studies of cold sprayed copper coating on the PVC polymer substrate," *Surface and Coatings Technology*, vol. 207, pp. 262-269, 2012/08/25/ 2012, doi: https://doi.org/10.1016/j.surfcoat.2012.06.086.

[27] A. Ganesan, M. Yamada, and M. Fukumoto, "Cold Spray Coating Deposition Mechanism on the Thermoplastic and Thermosetting Polymer Substrates," *Journal of Thermal Spray Technology*, vol. 22, no. 8, pp. 1275-1282, 2013/12/01 2013, doi: 10.1007/s11666-013-9984-x.

[28] X. L. Zhou, A. F. Chen, J. C. Liu, X. K. Wu, and J. S. Zhang, "Preparation of metallic coatings on polymer matrix composites by cold spray," *Surface and Coatings Technology*, vol. 206, no. 1, pp. 132-136, 2011/10/15/ 2011, doi: https://doi.org/10.1016/j.surfcoat.2011.07.005.

[29] A. S. Alhulaifi, G. A. Buck, and W. J. Arbegast, "Numerical and Experimental Investigation of Cold Spray Gas Dynamic Effects for Polymer Coating," *Journal of Thermal Spray Technology,* vol. 21, no. 5, pp. 852-862, 2012/09/01 2012, doi: 10.1007/s11666-012-9743-4.

[30] K. Ravi, Y. Ichikawa, T. Deplancke, K. Ogawa, O. Lame, and J.-Y. Cavaille, "Development of Ultra-High Molecular Weight Polyethylene (UHMWPE) Coating by Cold Spray Technique," *Journal of Thermal Spray Technology,* vol. 24, no. 6, pp. 1015-1025, 2015/08/01 2015, doi: 10.1007/s11666-015-0276-5.

[31] VRC Metal Systems. "Gen III™ Portable High-Pressure Cold Spray System,." https://vrcmetalsystems.com/gen-iii-portable-high-pressure-cold-spray-system/ (accessed May 8, 2022.

[32] DYMET. "Portable mobile Cold Gas Dynamic Spray Machine + Hot Sandblaster, 2 IN 1." http://dymet.ee/products-2/216-2/ (accessed May 8, 2022.

[33] MatterHackers Inc. "BASF Black Ultrasint PA6 X028 Laser Sintering Powder." https://www.matterhackers.com/store/l/basf-black-ultrasint-pa6-x028-laser-sintering-powder-sample-20kg/sk/MDNCLGK2 (accessed May 14, 2022.

[34] Sinterit. "PA12 Smooth." https://sinterit.com/materials/pa12-smooth/ (accessed May 14, 2022.

[35] M. B. Kennedy, J. R. Hawkes, A. T. Nardi, and M. A. Klecka, "Cold Spray Powder Feeders With In-situ Powder Blending," 2014. [Online]. Available: https://patents.google.com/patent/US10161048B2/en?q=Cold+spray+powder+feeders+in-situ+powder+blending&oq=Cold+spray+powder+feeders+with+in-situ+powder+blending

[36] D. Helfritch and V. Champagne, "Optimal particle size for the cold spray process," in *Proceedings of the international thermal spray conference*, 2006.

[37] T. Stoltenhoff, H. Kreye, and H. J. Richter, "An analysis of the cold spray process and its coatings," *Journal of Thermal Spray Technology,* vol. 11, no. 4, pp. 542-550, 2002/12/01 2002, doi: 10.1361/105996302770348682.

[38] V. F. Kosarev, S. V. Klinkov, A. P. Alkhimov, and A. N. Papyrin, "On some aspects of gas dynamics of the cold spray process," *Journal of Thermal Spray Technology,* vol. 12, no. 2, pp. 265-281, 2003/06/01 2003, doi: 10.1361/105996303770348384.

[39] T. W. Bacha, E. M. Henning, L. Elwell, F. M. Haas, and J. F. Stanzione, "Cold spray additive manufacturing of polymers: Temperature profiles dictate properties upon deposition," in *International SAMPE Conference and Exhibition 2020*, 2020.

[40] V. K. Champagne, D. J. Helfritch, S. P. G. Dinavahi, and P. F. Leyman, "Theoretical and Experimental Particle Velocity in Cold Spray," *Journal of Thermal Spray Technology*, vol. 20, no. 3, pp. 425-431, 2011/03/01 2011, doi: 10.1007/s11666-010-9530-z.

[41] Markforged Inc. "Mark Two (Gen 2)." https://shop.markforged.com/shop/s/product/mark-two-gen-2/01t1M00000MCEQgQAP (accessed May 22, 2022.

[42] Markforged Inc. "800cc Nylon White Filament Spool." https://shop.markforged.com/shop/s/product/800cc-nylon-white-filament-spool/01t1M00000LhNAiQAN (accessed May 22, 2022.

[43] Goodfellow. "Polyamide - Nylon 6 - Powder." https://www.goodfellow.com/us/en-us/displayitemdetails/p/am30-pd-000155/polyamide-nylon-6-powder (accessed May 22, 2022.

[44] D. Margerison and G. C. East, "CHAPTER 1 - INTRODUCTION," in *An Introduction to Polymer Chemistry*, D. Margerison and G. C. East Eds.: Pergamon, 1967, pp. 1-39.

[45] H. Che, X. Chu, P. Vo, and S. Yue, "Metallization of Various Polymers by Cold Spray," *Journal of Thermal Spray Technology*, vol. 27, no. 1, pp. 169-178, 2018/01/01 2018, doi: 10.1007/s11666-017-0663-1.

[46] G. Yang *et al.*, "Polymer Particles with a Low Glass Transition Temperature Containing Thermoset Resin Enable Powder Coatings at Room Temperature," *Industrial & Engineering Chemistry Research*, vol. 58, no. 2, pp. 908-916, 2019/01/16 2019, doi: 10.1021/acs.iecr.8b04698.

[47] G. Prashar and H. Vasudev, "A comprehensive review on sustainable cold spray additive manufacturing: State of the art, challenges and future challenges," *Journal of Cleaner Production*, vol. 310, p. 127606, 2021/08/10/ 2021, doi: https://doi.org/10.1016/j.jclepro.2021.127606.